JIMMA UNIVERSITY

JIMMA INSTITUTE OF TECHNOLOGY

SCHOOL OF GRADUATE STUDIES

FACULTY OF ELECTRICAL AND COMPUTER ENGINEERING

PAPR REDUCTION OF MIMO-OFDM SYSTEM USING MODIFIED CLIPPING AND TURBO CODING

By

Zemenu Addiss Melaku

This thesis is submitted to School of Graduate Studies of Jimma University in partial fulfilment of the requirements for the degree of

Master of Science

in

Communication Engineering

February 2022

Jimma, Ethiopia

JIMMA UNIVERSITY

JIMMA INSTITUTE OF TECHNOLOGY

SCHOOL OF GRADUATE STUDIES

FACULTY OF ELECTRICAL AND COMPUTER ENGINEERING

PAPR REDUCTION OF MIMO-OFDM SYSTEM USING MODIFIED CLIPPING AND TURBO CODING

By

Zemenu Addiss Melaku

Advisor: Dr. Kinde Anlay

Co-Advisor: Mr. Getachew Alemu
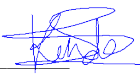
Submission Date: February,2022

Declaration

I declare that this thesis work, titled "PAPR reduction of MIMO-OFDM system using modified clipping and turbo coding," was written entirely by myself, with the exception of citations to other publications. This thesis has also never been submitted before for any other recognized or uncertified certification.

THESIS SUBMITTED BY:

Zemenu Addiss   ————————————   ————————————

                              Signature   Date

APPROVED BY ADVISORS:

ADVISOR: *Kinde Anlay (PhD)*   *16/02/2022*

                              Signature   Date

CO-ADVISOR: ————————————   ———————————-

                              Signature   Date

APPROVED BY THE BOARD OF EXAMINERS :

Approved by faculty of Electrical and computer engineering research thesis Examination members

1. ————————————   ———————   ———————-

       Chairman   Signature   Date

2. ————————————   ———————   ———————

       Examiner (Internal)   Signature   Date

3. *Fikreselam Gared (PhD)*   *Feb. 13/2022*

       Examiner (External)   Signature   Date

Acknowledgment

Abstract

Orthogonal frequency division multiplexing (OFDM) has been the most widely used multicarrier in recent mobile communication system due to its multiple advantages like high spectral efficiency, high data rate transmission over a multipath fading channel, simple implementation, and low receiver complexity. Currently, multiple-input multiple-output (MIMO) is combined with OFDM to boost spectral efficiency, work in a frequency selective environment, and enhance link reliability. Besides those crucial advantages, MIMO-OFDM system suffers from a high peak-to-average power ratio (PAPR) that originates from the superimposition of the number of sub-carriers with random amplitudes and phases. This high PAPR results in high power consumption by the power amplifier and high complexity in the design of analog to digital converter.

In this thesis work, modified clipping based PAPR reduction technique has been designed for MIMO-OFDM system and it is integrated with turbo channel coding scheme. In modified clipping method the MIMO-OFDM signal in each transmitter antenna has been clipped into different threshold values using a settle quantization levels, step size value and number of clipped high peak envelope signals as parameters. A powerful turbo channel coding enables to reduce the clipping and channel fading distortion with the aids of iterative decoding using space-time block code (STBC) bit-wise soft detection values as input. This allows to achieve better bit error rate (BER) performance. The PAPR and BER of the turbo code based modified clipping STBC MIMO-OFDM have been verified using Matlab software for the selected numerical values of modified clipping parameters. In addition, the designed modified clipping performance has been compared to the conventional clipping performance using PAPR and BER metrics.

The simulation result demonstrated that the modified clipping having comparable PAPR performance to that of the conventional clipping has better BER performance. Using modified clipping method having 25% of clipped high peak envelopes, 5 quantization levels, and 0.05 step size with 1/3 rate turbo code the PAPR performance can improve by 69.09%, 71.05%, and 72.65% for a sequential

sub-carrier length of 128, 256, and 512 over its respective original PAPR performances. Under those modified clipping parameters value with different turbo code iteration the remarkable bit energy to noise power spectral density ratio E_b/N_0 gain has been obtained at a given BER value.

Keyword: **MIMO-OFDM, Turbo code, Modified clipping, PAPR, BER**

Contents

List of Figures

List of Tables

Abbreviations

ADC	Analog to Digital Converter
AWGN	Additive White Gaussian Noise
BER	Bit Error Rate
BPSk	Binary Phase Shift Key
CARI	Cross Antenna Rotation and Inversion
CC	Convolutional Code
CCDF	Complementary Cumulative Distribution Function
CP	Cyclic Prefix
FDM	Frequency Division Multiplexing
FFT	Fast Fourier Transform
HPA	High Power Amplifier
IBO	Input Back Off
IFFT	Inverse Fast Fourier Transform
LDPC	Low Density Parity Check
LLR	Log Likelihood Ratio
MAP	Mximum A Posteriori
MCM	Multi Carrier Modulation
MIMO	Multiple Input Multiple Output
ML	Mximum Likelihood
MSP	Multiple Signaling Probabilistic
NSC	Non Systematic Code
OFDM	Orthogonal Frequency Division Mutliplexing
PAPR	Peak to Average Power Ratio
PCC	Parallel Concatenated Convolutional

PTS	**P**artial **T**ransmit **S**equence
QAM	**Q**uadrature **A**mplitude Modulation
QPSK	**Q**uadrature **P**hase **S**hift **K**ey
RSC	**R**ecursive **S**ystematic Convolutional
SC	**S**ystematic **C**ode
SCM	**S**ingle **C**arrier Modulation
SD	**S**ignal **D**istortion
SI	**S**ide Information
SLM	**SL**ective **M**apping
STBC	**S**pace **T**ime **B**lock **C**ode
SOVA	**S**oft **O**utput **V**iterbi **A**lgorithm
TC	**T**urbo **C**ode

Chapter 1

Introduction

1.1 Background

The early digital communication systems were based on a single carrier modulation (SCM) scheme, in which the entire bandwidth has been designated to one radio channel. In SCM systems the signal highly susceptible to the influence of deep fading in a multipath channel. Multicarrier modulations have been then presented as a good alternative to combat this multipath fading effect in SCM. In the multicarrier modulation (MCM) technologies the available bandwidth divides into multiple sub-channels so that it converts the serial high rate data stream to multiple low rate sub-streams transmitted in parallel over each sub-channel [1],[2]. Recently, different MCM candidate waveforms like orthogonal frequency division multiplexing, filter bank multicarrier offset quadrature amplitude modulation [3], generalized frequency division multiplexing [4], universal filtered multicarrier [5], and filtered orthogonal frequency division multiplexing [6] were being developed to fulfill 5G network requirements.

Among those candidate physical layer waveforms as of now, OFDM is the most popular one in many standards and applications. OFDM has been supported by many European standards and standardization groups like IEEE 802.11 and IEEE 802.16 [1], [7–11]. In OFDM parallel transmission of lower data rate streams

using several orthogonal subcarriers allows to increase the symbol duration, thus decreasing the prorated amount of dispersion in time resulting from the multipath delay spread.

In addition to MCM, the demands of wireless communication evolved to multiple-input multiple-output technology. MIMO technology enables to achieve the system link reliability through spatial diversity and the high data rate through spatial multiplexing. In a diversity system, fading for each link between a pair of transmitting and receiving antennas is considered to be independent and the same information travels through diverse paths. As a result, the probability of accurate detection of the information increases. In the transmitter, spatial diversity has been accomplished by utilizing space-time block code. STBC relies on coding of the data symbols across space and time to extract diversity and also it offers simple decoding with the use of a maximum likelihood detection algorithm at the receiver [12–14]. As demonstrated in [13] and [15] practically MIMO in the wireless communication system is frequency selective. To solve this frequency selective nature of MIMO, a promising combination has been exploited between MIMO and OFDM.

In spite of its advantages, OFDM suffers to high peak-to-average power ratio originates from the superimposition of subcarriers with random amplitudes and phases. High PAPR is also an issue in MIMO-OFDM systems [15], [16]. Since the design of system components like a high power amplifier (HPA) with a large linear region operating point is impractical and prohibitively high cost, a practical MIMO-OFDM implementation must consider measures to reduce the high PAPR efficiently.

This thesis work mainly focuses on the clipping version of the PAPR reduction technique, since clipping is compatible with the MIMO-OFDM system and also it has less complexity. To attain better PAPR reduction gain and BER performance gain many research works were conducted in clipping, clipping and filtering, iterative clipping and filtering as well as in a combination of those with other PAPR techniques. At all clipping introduces out-band radiation as well as in-band signal

distortion, which results in signal interference in adjacent channels and BER performance degradation respectively. The out-band radiation problem in clipping has been solved by filtering but the in-band distortion is still an open problem. The BER limitation of clipping has been more prominent in the high order diversity MIMO-OFDM system, so for the sake of BER performance, the clipping threshold usually settles too large, thus resulting in less PAPR reduction gain.

To combat this limitation, the application of turbo channel coding has been applied to the designed modified clipping PAPR reduction technique for the MIMO-OFDM system. In turbo-based modified clipping MIMO-OFDM system, the selected high peak envelopes have been clipped in successive manners using the numbers of quantization levels and a preset step size value. For bit-wise soft STBC detection the log maximum a posteriori probability (Log-MAP) algorithm has been utilized, since Log-MAP algorithm has sub-optimal performance with the reasonable moderate complexity [17].

Using STBC bit-wise soft detection values as input turbo decoder works in an iterative manner to find out the best estimate of the received sequence, so it results in better BER performance for the proposed modified clipping MIMO-OFDM system. In this thesis work, the system performance has been evaluated using complementary cumulative distribution function (CCDF) and BER metrics with different numbers of quantization levels, step size values, sub-carriers, number of clipped high peak envelopes, and turbo iterations. In addition, the designed modified clipping performance has been compared to the conventional clipping method under PAPR and BER metrics.

1.2   Statement of the Problem

The instantaneous peak power is a crucial parameter since it determines the power level that the power amplifier in the transmitter must be capable of supplying. This instantaneous peak power of a wireless communication system depends on the encoded information symbols. Since the MIMO-OFDM system has randomly

varying symbols a highly fluctuating instantaneous peak power has occurred. The high instantaneous peak power results in high PAPR. Having high PAPR leads HPA operating beyond the normal linear level, thus introducing distortion of the input signal and system performance degradation. To overcome the non-linear operating point of HPA large back-off, large dynamic range digital-to-analog converter (DAC), and linear converters are required. However, back-off is determined by the PAPR value. As a result, high PAPR requires a large back-off. This leads power deficiency in the amplifier.

A large back-off also requires a high-precision DAC which is high cost and high power consumed. The requirement of the large dynamic range of the power amplifiers and heavily linear converters to accommodate large PAPR values result in an additional cost to the system. In general, due to high costs and inefficient works of components like linear converts and DAC, the design of linear HPA in the presence of high PAPR will be impractical. Moreover, high PAPR makes the HPA enter in its saturation region, this causes in-band distortion that results in a degradation of the BER performance and out-band distortion that results in adjacent channel interference.

1.3   Objectives of the Research

1.3.1   General Objective

The general objective of this thesis is to design a simple modified clipping technique and to combine it with turbo channel coding for PAPR reduction of the MIMO-OFDM system.

1.3.2   Specific Objectives

The specific objectives of this thesis include:

- To evaluate the PAPR and BER of the MIMO-OFDM system with and without turbo coding.

- To evaluate the PAPR of the MIMO-OFDM system with conventional clipping at different clipping ratio levels.

- To evaluate the effects of conventional clipping on the BER performance of the MIMO-OFDM system.

- To evaluate the effects of modified clipping quantization levels on the PAPR and BER performances of the MIMO-OFDM system.

- To evaluate the effects of modified clipping step size values on the PAPR and BER performances of the MIMO-OFDM system.

- To evaluate the effects of modified clipping high peak clipped signal envelopes on the PAPR and BER performances of the MIMO-OFDM system.

- To combine modified clipping with turbo code for enhancement of MIMO-OFDM system BER performance.

- To analysis the computational complexity of the proposed system work.

1.4   Methodology

In this thesis work, a modified clipping-based PAPR reduction technique with a powerful turbo channel coding has been proposed for the MIMO-OFDM system. The first task of this study is to review distinctive literature about channel coding especially turbo coding, MIMO-OFDM system, PAPR effects, and PAPR reduction techniques in the MIMO-OFDM system to build up a solid understanding for the thesis work. The subsequent task is to select the less complex PAPR reduction technique i.e. clipping and to demonstrate its effect on the PAPR and BER performance at different clipping threshold levels. After that, with the aim of reduction of clipping limitation a new modified clipping PAPR reduction technique has been designed. In modified clipping the selected peak envelopes have

clipped in successive manner using the settle step size value and numbers of quantization levels. This allows better BER performance as compared to conventional clipping. Although, modified clipping results in better BER performance, like conventional clipping the trade-off exists in between BER performance and PAPR reduction gain. To compromise BER and PAPR performance trade-off in a better way turbo code has been applied. The integration of turbo code to the designed modified clipping technique enables to the reliable bit-wise soft information estimation. As a result, the turbo code based modified clipping better BER and PAPR performance trade-off over the conventional clipping MIMO-OFDM system and the uncoded MIMO-OFDM system. Meanwhile, the designed modified clipping MIMO-OFDM system computational complexity with a reference of conventional clipping has been analyzed.

1.5   Significance of Research

This thesis has numerous significance for the MIMO-OFDM system by reducing its high PAPR. The reduction of high PAPR using modified clipping technique has allowed achieving better HPA efficiency, better link coverage, and extended mobile battery life. In addition, the use of modified clipping technique for high diversity MIMO-OFDM system results in better BER performance over conventional clipping technique. Furthermore, a combination of modified clipping with powerful turbo code in the MIMO-OFDM system results in a significant BER performance gain over the MIMO-OFDM system alone. As a result, a better compromise in the trade-off between PAPR reduction gain and BER performance has been investigated for the MIMO-OFDM system using a combination of modified clipping and turbo code.

1.6   Scope of Research

A number of tasks have been accomplished in this thesis work. In the first task, the MIMO-OFDM system performance in terms of PAPR and BER metrics has been evaluated. To reduce the crucial high PAPR problem of MIMO-OFDM clipping technique has been considered. Meanwhile, clipping with a small clipping ratio reduces high PAPR in a significant manner it suffers BER degradation. To mitigate BER degradation a designed modified clipping technique with the integration of turbo code has been proposed. For a designed modified clipping MIMO-OFDM system the effect of quantization levels, value of step size, and numbers of clipped high peak envelopes on PAPR and BER performances has been evaluated. While evaluating the proposed BER performance the assumption of perfect channel state information at the receiver has been taken. In addition, the effects of filtering have not been considered on system metrics performance.

1.7   Contributions of Research

The main contribution of this thesis work is to address the high PAPR challenge in the MIMO-OFDM system. The key limitation in this system is the existence of an effective PAPR reduction method. In the most existing method, the trade-off exists in between the BER performance and the PAPR reduction gain. To compromise this trade-off in a better manner a simple modified clipping has been designed and it is integrated with turbo channel coding. The main contributions in this thesis study have been summarized as follows:

- Design of modified clipping with comparable PAPR and slightly better BER performances to that of conventional clipping.

- Comparison of the designed system performance with the existing conventional clipping method through simulation results.

- To show the effect of the numbers of quantization levels, step size value, and the numbers of clipped high peak envelopes on performance metrics.

- To combine modified clipped and turbo coding in the MIMO-OFDM system.

- To analysis the computational complexity of the proposed system.

1.8 Thesis Outline

The rest of this thesis has been organized as follows: chapter two presents the most recently proposed PAPR techniques for the MIMO-OFDM system which have been suggested by different researchers. Chapter three provides the basic overview of the several topics and concepts that have been covered over the course of this thesis. It presents an introduction about Channel coding especially turbo coding, OFDM, STBC MIMO-OFDM, PAPR effects, and PAPR reduction techniques. Chapter four presents the designed modified clipping and turbo code based proposed system design and methodology. To provide bit-wise soft input values for turbo decoder the STBC detection using Log-MAP analysis is also present. In addition, the proposed system's computational complexity has been analyzed in this chapter. In Chapter 5, the simulation results of the proposed system using PAPR and BER performance metrics have been discussed in detail. Finally, in chapter 6 the conclusions and the recommendations of the thesis work have been presented.

Chapter 2

Literature Review

As illustrated in the introduction, high PAPR is the main problem in OFDM as well as in the MIMO-OFDM system and if this is not solved it may result in the loss of system advantages. To mitigate such problems a number of methods have been done. According to [15] PAPR reduction techniques can be classified into four broad classes: signal distortion techniques, multiple signaling and probabilistic schemes techniques, coding techniques, and hybrid techniques.

Signal distortion (SD) techniques reduce high peaks in the OFDM signal by distorting the signal before being amplified by HPA. The commonly used SD techniques in the OFDM system includes companding [15], [18–20], clipping [21–23], peak cancellation [24], and peak windowing [25]. Some of those methods are adopted for the MIMO-OFDM system.

A PAPR reduction method that combines SD μ-law companding with polar Codes has been presented in [18]. Here nonlinear μ-law companding is used to compress high dynamic range signals at the transmitter and to recover those compress signals at the receiver by applying its inverse. To combat undesirable effects of compression and noise in the transmission channel polar code was applied. The result in PAPR and BER metrics has been shown at varies μ-law compression values and sub-carrier lengths with μ-law de-companding and without μ-law de-companding operation at the receiver. The simulation result demonstrated that the high PAPR

has reduced proportionally with the increase of μ values at a cost of BER performance. The best PAPR value (i.e. $\approx 3dB$) was obtained at $\mu = 255$ for quadrature phase-shift keying modulation(QPSK). Also, the BER of the MIMO-OFDM system using polar code without μ-law de-companding outperforms the system with μ-law de-companding. In addition to this, the author concludes that the proposed system results in a better PAPR performance as compared with partial transmit sequence and selective mapping PAPR reduction techniques. Although PAPR reduces in a good manner, BER performance with μ-law de-companding has deteriorated as compared to the original MIMO-OFDM system. Further apart from this the impacts of μ-law companding on the BER performance of the system having more than two receiver antennas has not been investigated.

Xiaodong Zhu has proposed another SD-based PAPR reduction technique using clipping for the MIMO-OFDM system [21]. Unlike conventional clipping operation has been applied after space-time block coding in this work clipping has applied before space-time block coding. The purpose of the new scheme is to reduce the BER loss with the same PAPR reduction ability to that of conventional clipping. The designed system BER and PAPR performances were proved using simulation results and theoretical analysis. Although, this method has slightly better BER still the loss is more and still under question especially at a low clipping ratio (i.e. at good PAPR reduction gain).

In [22] and [23] the adaptive clipping based PAPR reduction technique were investigated for MIMO-OFDM and OFDM systems respectively. In presented work, the high peak envelopes were clipped successively. The simulation results reveal that the proposed clipping technique results in better performances over convention clipping technique in power spectral density, PAPR reduction and BER aspects. Using nine reduction factors (i.e 10 clipped high peak envelopes) around $4dB$ PAPR reduction gain achieved for 2×1 OFDM system. Although, adaptive clipping results in better BER and PAPR reduction gain performance its effect for high diversity order STBC OFDM system were not shown. In addition the effect of the numbers of selected high peak envelopes were not evaluated and at large

numbers of selected peak envelopes i.e. better PAPR reduction gain the BER performance severely deteriorates.

The second class of PAPR reduction technique i.e. multiple signaling and probabilistic (MSP) scheme decreases the high PAPR occurance by using scramble codes and modifying different parameters of the OFDM signals. In this technique, multiple candidate signals containing the same information have been generated and the one with the lowest PAPR has been selected for transmission. Multiple signaling and probabilistic technique includes tone reservation [26], tone injection [27], precoding transform techniques [28], selective mapping (SLM) [13], [29–31], partial transmit sequence (PTS) [32],[33], active constellation extension [34], interleaving [35] etc.

The PAPR reduction technique using a class of MSP technique i.e. SLM with low complex time-domain cyclic was examined for the MIMO-OFDM system [29]. In the system, signal candidates have been generated by summing the original OFDM signal with its cyclically shifted version, and then the signal candidate with the lowest PAPR has been transmitted. Further to complexity reduction, the loss of data rate is eliminated by removing the transmission of overhead (i.e. side information) to the receiver. As examined in the paper the estimation of cyclic shift in the receiver has been required to investigate the transmitted data. This results in system BER performance losses as it depends on the correct estimation of cyclic shift. Also, the PAPR reduction gain is not satisfactory i.e. 2 *dB* only.

Another MSP method that combines random and interleaved segmentation PTS schemes has been proposed by M. Wang for the MIMO-OFDM system [33]. The author's main intention was the reduction of conventional random segmentation PTS complexity and it reduces by 41.1% for 128 sub-carriers using 4 subblocks. Also, the goal has been achieved the hybrid PTS scheme results in some penalty on PAPR reduction gain as compared to the random segmentation which has the best PAPR reduction performance over other versions of PTS. Therefore, sufficient PAPR reduction gain has not been obtained using this hybrid subblock segmentation PTS scheme. In addition, the requirement of side information (SI) at the

receiver side introduces losses in the data rate and bandwidth efficiency of the system.

The coding PAPR reduction techniques (including linear block codes, convolutional codes, and concatenated codes) have been concerned with choosing the codewords that minimize the high PAPR. The coding technique is mainly used for two purposes. The first one is for BER improvement and the other one is for both PAPR reduction and BER improvement. But in the second purpose, it suffers a complexity rise with sub-carrier length as to find out the best codewords with minimum PAPR.

In [36], a linear coding type called low density parity check (LDPC) has been proposed for PAPR reduction of the MIMO-OFDM system. The result compared with the available time existed PTS, SLM, turbo code, and convolutional code and the author concludes that LDPC results in a better PAPR reduction gain. However, searching for the best codeword with minimum PAPR for transmission introduces complexity and latency especially for large data transmission. This latency may not be tolerable in real-time data transmission. In addition to latency and complexity, it also requires accurate side information to know which codeword has been selected and thus may introduce BER penalties like PTS and SLM.

In the hybrid techniques, two or more methods are combined to achieve desirable PAPR reduction. The hybrid methods have been considered as a better choice for PAPR reduction since it possesses the advantages of both techniques used in hybridization with increases in complexity. For example, PTS has proposed with interleaving and pulse shaping method [37], with SLM [38], with turbo codes and Golay codes [39] etc.

A hybrid PAPR reduction technique that combines three methods namely convolutional code, successive suboptimal cross-antenna rotation and inversion (CARI), iterative modified μ-law companding and filtering has been done in [15] for the MIMO-OFDM system. In this method, remarkable PAPR reduction was achieved with comparable BER performance to that of the MIMO-OFDM system alone. In

this hybrid technique, the complexity and PAPR performance depend on partitioned subblocks. The CARI method requires additional SI that leads to a reduced data rate. In addition, SI has impact on the BER performance if it is not correctly recovered at the receiver.

Generally, an effective PAPR reduction technique that fulfills the PAPR and BER requirements at once has not been investigated. In most existing work the system with PAPR reduction technique has some BER performance loss over a system without PAPR reduction technique i.e trade-off exists in between PAPR reduction gain and BER performance. As a result, in this thesis work the simple modified clipping technique with more effective forward error control technique (i.e. turbo coding) has been proposed to achieve remarkable PAPR reduction with outstanding BER performance. The designed modified clipping technique of this thesis study is the extension of the work investigated in [22]. The designed modified clipping technique, unlike of [22] the MIMO-OFDM selected high peak envelopes have been clipped using the numbers of quantization levels with a settle step size value. This enables the designed modified clipping at a comparable PAPR reduction gain with conventional clipping and adaptive clipping technique proposed in [22] to has BER advantage for high diversity order STBC MIMO-OFDM system. In addition, turbo code plays a major role in the BER enhancement of the clipped and fading signal with some penalties of spectral efficiency and overall system complexity.

Chapter 3

MIMO-OFDM Overview

3.1 Introduction

In this chapter, an overview of the MIMO-OFDM system has presented. Figure
3.1 shows the schematic diagram of the channel code-based MIMO-OFDM system.
The system basically consists of a channel encoder, digital modulator, space-time
block code, OFDM modulator, and each of its inverse operations at the receiver
side. At the transmitter side shown in figure 3.1(a), the generated data bit se-
quences have been encoded by channel code or maybe left uncoded i.e. uncoded
MIMO-OFDM and then every set of m coded bits or uncoded bits are mapped
to one of the M=2^m size complex symbols. The digital modulator can be BPSK,
QPSK, or QAM. Then after the complex symbols from the digital modulator pass
to the STBC encoder.

The STBC encoder performs some operation in such a way that the linear combi-
nations of the incoming symbols and their conjugates are able to transmit by N_t
transmitter antennas at a certain time. For the STBC encoding symbols along
with each transmitter antenna,i (i = 1, 2, ... , N_t) OFDM modulation has ap-
plied and finally, the modulated signals have been transmitted by N_t transmitter
antennas. On the receiver side, each of the corresponding reverse processes has

been carried out as shown in figure 3.1(b). In the next subsections, the details of each block diagram has been examined.
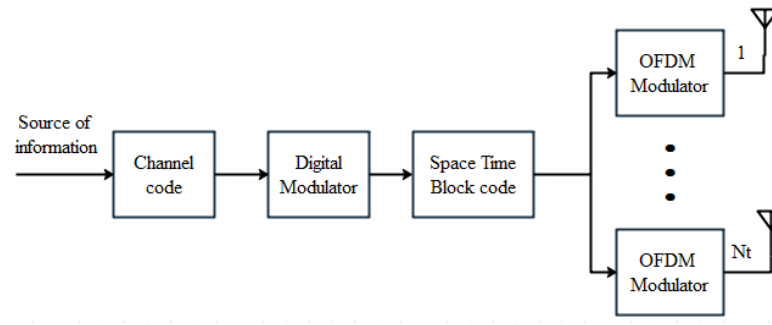
(a) MIMO-OFDM transmitter
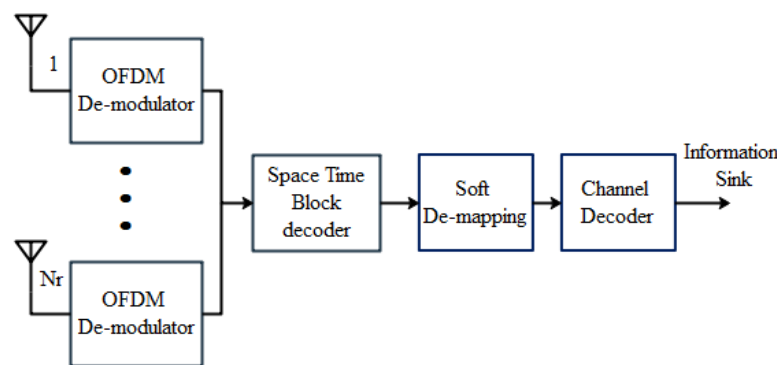
(b) MIMO-OFDM receiver

FIGURE 3.1: Block diagram of MIMO-OFDM transceiver.

3.2 Channel Coding

In digital communication system, the major concern is to minimize the error probability at the receiver end with efficient use of the available resources. To achieve this low error probability channel code has been incorporated. By adding some redundancy bits to the transmitted data, the original data at the receiver hopefully can recover. Many early channel coding applications were developed for deep space and satellite communication systems [40], [41]. In addition to deep space and satellite communication systems recently coding technologies predominates in numerous scientific, military, and commercial applications [42–44]. Today different channel codes are available with different performance and areas of applications. Generally, depending on the ways of the redundancy to the information data sequences channel coding can be classified as block code and convolutional code.

In block coding, memoryless operations in the encoder and decoder are carried out for independent data blocks. Whereas in convolutional coding the continuous data stream encoding and decoding operations depend not only on the current data but also on the previous data. Depending on the message sequences in codeword (codeword implies bit sequences after redundancies added) both block code and convolutional codes can be further classified as [22]:

- Non systematic code (NSC)

- Systematic code (SC)

Figure 3.2(a) shows that in a non-systematic convolutional code with two memory D1 and D2 redundancies are implicitly embedded in the codewords so direct extraction of the original message from the decoded codeword is not possible at the receiver. For systematic convolutional code redundancies are explicitly appended to the message sequences i.e. the input sequences can reproduce without altering in the output codeword as shown in figure 3.2(b) by output1. In this case, the original data and the parity data are separated so the receiver can directly extract the original data from the decoded codeword.

(a) Non-systematic (b) Systematic
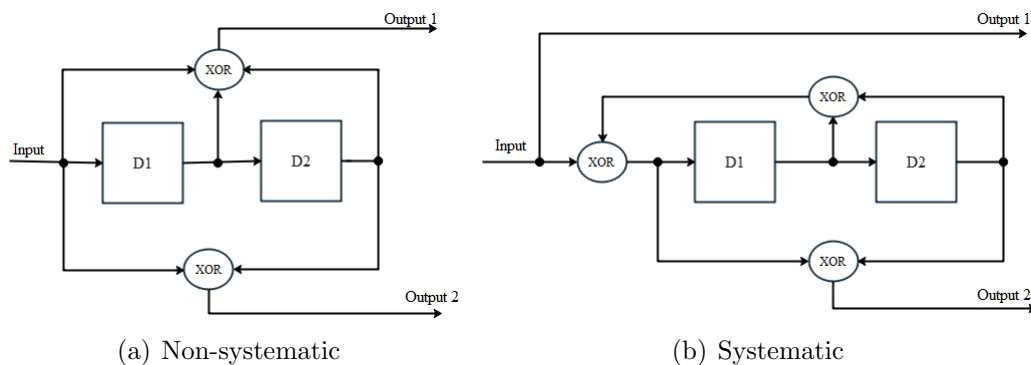
FIGURE 3.2: Non-systematic and systematic convolutional code structures.

Before discussing the details of turbo coding (TC) and some highlights of convolutional code (CC) let's discuss some basic terms that have been needed frequently.

- **Memory order (L):** it is the maximum number of shift register stages in the path to output bit. For example in figure 3.2 we have L=2, that is D1 and D2.

- **Constraint length (K):** it is the length of the convolutional encoder i.e. the maximum number of input bits that output can depend on. Constraint length K is given by $K = L + 1$.

- **Code rate (R):** it is a ratio of the number of k bits fed into the channel encoder to the number of n bits output from the channel encoder i.e. $R = \frac{k}{n}$.

- **Coding gain:** it indicates the improvement in the ratio of energy per bit of information to noise power spectral density E_b/N_o with respect to a given BER reference value.

3.2.1 Convolutional Code

Knowing the convolutional encoder and decoder principle is the main strategy to understand the working principle turbo code. After being introduced in 1955 by Elias, CC has gained vast popularity in satellite communications, GSM, UMTS, IS-95, and CDMA2000 standards for mobile communications [45]. This popularity is mainly due to its good performance and flexibility to achieve different coding rates as it compares with block coding.

3.2.1.1 Convolutional Encoder

In CC a continuous sequence of information bits is mapped into a continuous encoder output sequence of bits. As the CC contains memory, the n-tuple output generated by the encoder is a function of both the u-tuple current input bits and L previous tuple bits. Mostly CC specified using the number of input bits k to the encoder at a time t, the number of output bits n from the encoder for a given k and constraint length K as (K, k, n). Now let consider (3, 1, 2) a non-systematic CC given in figure 3.2(a) with a binary data stream $u(1)\,u(2)\,u(3)\,\ldots$ fed into shift register with $L = 2$. The coded output data streams output 1 and output 2 are given by:

$$
\begin{aligned}
\text{output 1 } (n) &= u(t) \oplus u(t-1) \oplus u(t-2) \\
\text{output2}\,(n) &= u(t) \oplus u(t-2)
\end{aligned}
\tag{3.1}
$$

Where $u(t)$ is the current input bit of the encoder and $\oplus$ denotes modulo 2 addition. The two coded outputs are may be puncturing according to a certain pattern if necessary and then they are multiplexed to get a single-coded output data stream. Commonly the encoder has been described using generator polynomial that represents the generation of each output bit from the input bits. By considering the left most spot in the binary number representation as to the current input the rightmost spot is the oldest input that still remains in the shift register for Figure 3.2(a) the generator polynomial given by:

$$G = [g_1, g_2] = [111, \ 101] \tag{3.2}$$

Using binary representation given in (3.2) an octal representation of 7 and 5 have gotten for g_1 and g_2 respectively. Similarly the generator polynomial for systematic CC given in figure 3.2(b) can be written as:

$$G = \left[1, \frac{g_1}{g_2}\right] \tag{3.3}$$

Where 1 denote the systematic output and g_1, g_2 denotes the feed-back to the input of the recursive SC encoder and the feed-forward output respectively.

3.2.1.2 Convolutional Decoder

Convolutional decoding is the process of searching for the path that an encoder has traversed. CC can be decoded using either maximum-likelihood (ML) or the Viterbi algorithm. Viterbi decoding algorithm involves finding the path having the largest metric through the trellis by comparing the metrics of all branch paths entering each state with the corresponding received vector. Viterbi decoding can be:

- Hard Viterbi decoding

- Soft Viterbi decoding

In hard-decision decoding, from each received signal the decoder decides whether the transmitted signal is zero or one. Unlike hard-decision decoding in soft decision the received noisy signals are not assigned to zero's and one's combination, rather side information is generated by the receiver bit circuitry and this gives additional confidence about the received information to the decoder. Moreover, soft decoding uses more bit metrics, and this results in a better coding gain over the hard decision Viterbi decoding algorithm.

3.2.2   Turbo Code

Turbo code is one class of concatenated convolutional code and it gains more attention in the field of research after it was introduced. This is due to its Shannon capacity approaches performance [17], [40], [46]. Concatenation in TC can be serial, parallel, or a combination of both parallel and serial. In serial concatenation, each information bit encoded by each component encoders in a sequential manner thus resulting in much more delay, especially for large data sequences. As the result, parallel concatenation is preferable. The choice of the interleaver is crucial in the code design to make the outputs of the two encoders uncorrelated from each other, thus yielding more reliability while decoding. Turbo decoder uses soft input values and results in soft-output values for the decoded data sequences.

3.2.2.1   Turbo Encoder

The Parallel concatenated convolutional (PCC) turbo encoder consists of two identical recursive systematic convolutional (RSC) encoders separated by the interleaver and concatenated in a parallel fashion shown in Figure 3.3. Each RSC component encoder (for example the one shown in Figure 3.2(b)) having a rate $R = 1/2$ produces a systematic output that is equivalent to the original information bit sequences and a stream of parity bit sequences. As indicated in Figure 3.3, the input bit sequences directly get into the first RSC encoder, whereas the second RSC encoder takes the scrambled version of the input bit sequences using

interleaver. The performance of turbo code mainly depends on the effectiveness of interleaver design.
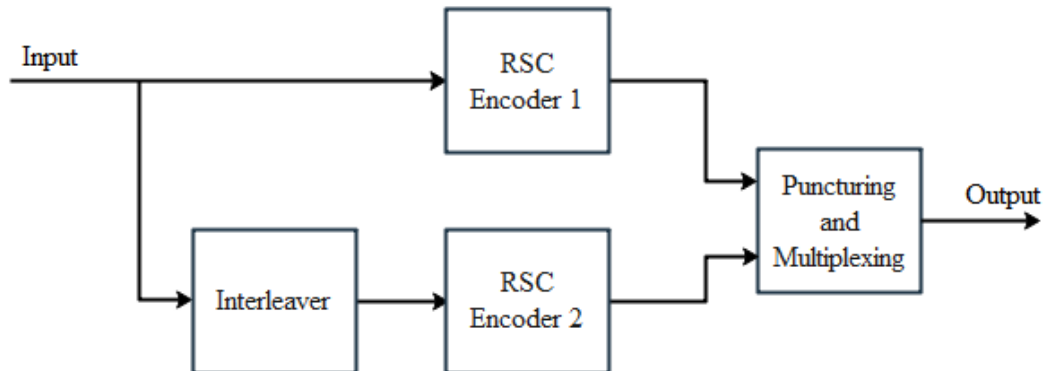
FIGURE 3.3: Block diagram of PCC turbo encoder.

In [40] random interleaver outperforms both the block and reverse block interleavers as the result of its better free distance codewords (i.e. large hamming distance). Therefore, in this study, random interleaver has been used. The systematic outputs from the two RSC encoders are identical to each other (although ordered differently). Therefore, by discarding the systematic sequences from the second component encoder the overall code rate becomes $R = 1/3$.

Also, a wide range of coding rates can be realized by puncturing the two parity sequences (since puncturing of systematic bits degrades coding performance so its puncturing is not recommended) using certain puncture patterns before being transmitted along with the original information sequence [47]. Then, the punctured parity bit sequences and systematic bit sequences are multiplexed together for transmission. Although more puncturing of the parity bit sequences can achieve a code rate approach to one, this deteriorates the error-correcting ability of code. Therefore, always a trade-off exists between coding rate and error-correcting performance. Finally, an M-ary modulator maps a block of m binary digits from the multiplexed bit sequences into one of M the possible complex symbols, where $M = 2^m$.

3.2.2.2 Turbo Decoder

A special type of algorithm that accepts soft values as input and gives soft values output has been used for turbo decoding. These soft inputs and outputs provide not only an indication of whether a particular bit was a 0 or a 1, but also the probability that the bit has been correctly decoded. As shown in Figure 3.4 turbo decoder consists of two component decoders. The first component decoder decodes the noisy received sequences from the first component encoder, and second component decoder decodes the noisy received sequences from the second component encoder.
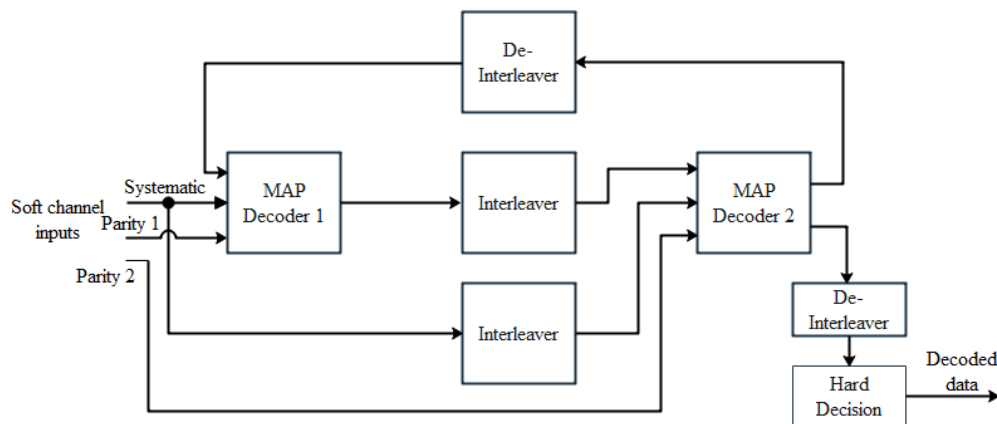
FIGURE 3.4: Block diagram of turbo decoder.

Each decoder takes three inputs: the systematically encoded channel output bits, the parity bits transmitted from the associated component encoder, and the information about the likely values of the bits concerned (i.e. a-priori information). Using these input values the decoder provides the decoded output bit sequence and also the associated probabilities for each bit that has been correctly decoded. This is known as soft outputs. Soft output values are represented in terms of log likelihood ratios (LLRs). The sign of LLR indicates whether the decoded bit is being 0 or 1 and its magnitude tells about the probability of correct decision of the corresponding bit. The turbo decoder operates through exchanges of extrinsic information in between componenet decoders . TC decoding algorithm can work using any of the following as a component decoder [17]:

- Soft Output Viterbi Algorithm (SOVA)

- Maximum A posteriori Probability (MAP)

Since the SOVA decoding algorithm is not commonly used for TC due to its inferior performance. As a result, in the next subsection, only the detail of the MAP algorithm and its modified version has been presented.

3.2.2.3 MAP Decoding Algorithm

MAP uses some bits before and after the current bit in the trellis diagram to estimate the most likely transmitted data bit. LLR of the input data bit u at time t defined as a-priori probability $pr(u)$ of the bit taking its two possible values i.e.

$$L(u_t) = \ln \frac{pr(u=1)}{pr(u=0)} \tag{3.4}$$

LLR simplifies the passing of information from one component decoder to the other in the iterative transmitted bit estimation. From Figure 3.5 y is the M-ary modulated data symbol sequences from codeword sequences x and r be the corresponding noisy version of y in the receiver which is given by:

$$r = hy + \eta \tag{3.5}$$

Where h is the channel fading coefficient and η is the AWGN with variance σ^2.
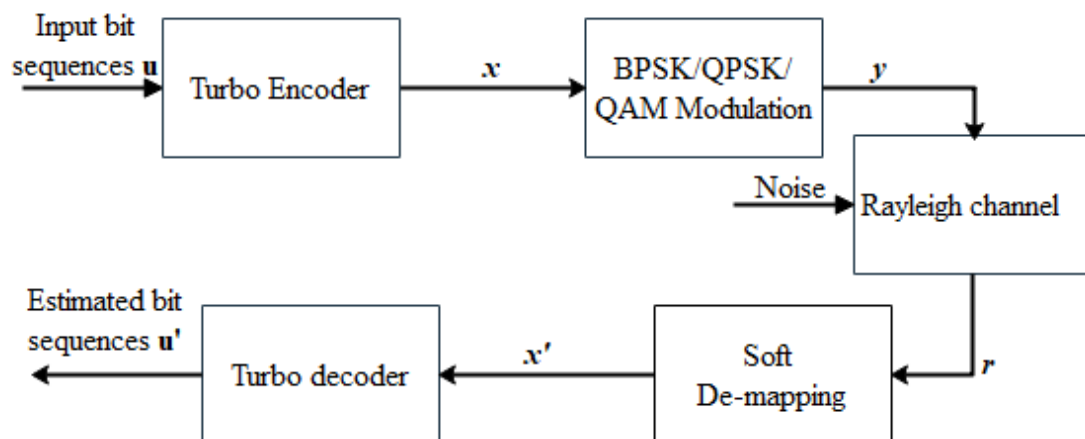
FIGURE 3.5: Simplified block diagram of communication system with TC.

Now under the condition that a sequence r has been received, the l$^{\text{th}}$ bit-wise soft input of the turbo decoder using m-tuple bit symbol y at time t express as:

$$L\left(x'_{l,t}/r\right) = \ln\left(\frac{\sum_{y_{l\Rightarrow 1}} pr\left(y_l/r\right)}{\sum_{y_{l\Rightarrow 0}} pr\left(y_l/r\right)}\right) \tag{3.6}$$

Where l = 1, 2, . . .m denote the lth position bit sequence corresponding to the symbol y and $y_{l\Rightarrow 1}$, $y_{l\Rightarrow 0}$ denotes the symbol subset of y with the lth bit being 1 and 0 respectively. Using conditional Bayes probability:

$$pr\left(A/B\right) = pr\left(B/A\right)\frac{pr\left(A\right)}{pr\left(B\right)}$$

$L\left(x'_{l,t}/r\right)$ can be express using (3.7).

$$L\left(x'_{l,t}/r\right) = \ln\left(\frac{\sum_{y_{l\Rightarrow 1}} pr\left(r/y_l\right)}{\sum_{y_{l\Rightarrow 0}} pr\left(r/y_l\right)}\right) + \underbrace{\ln\left(\frac{\sum_{y_{l\Rightarrow 1}} pr\left(y_l\right)}{\sum_{y_{l\Rightarrow 0}} pr\left(y_l\right)}\right)}_{a-priori\ information} \tag{3.7}$$

Assuming the event of selecting $y_l \in \{0,1\}$ in transmission symbol is equiprobable. This follows a-priori information about y_l which is obtained from other independent sources like channel decoder be constant. Assume a perfect channel state information h is available at the receiver, then the conditional pdf $pr\left(r/y_l\right)$ in [48] given by:

$$pr\left(r/y_l\right) = \frac{1}{\sqrt{2\pi\sigma^2}}\exp\left(-\frac{1}{2\sigma^2}\left\|r - hy_l\right\|^2\right) \tag{3.8}$$

Using $pr\left(r/y_l\right)$ the LLR given in (3.7) can rewrite as:

$$L\left(x'_{l,t}/r\right) = \ln\left(\frac{\sum_{y_{l\Rightarrow 1}} \exp\left(-\frac{1}{2\sigma^2}\left\|r - hy_l\right\|^2\right)}{\sum_{y_{l\Rightarrow 0}} \exp\left(-\frac{1}{2\sigma^2}\left\|r - hy_l\right\|^2\right)}\right) \tag{3.9}$$

3.2.2.4 Log-MAP and Max-Log-MAP Decoding Algorithms

The MAP algorithm in (3.9) contains many exponential terms in both numerator and denominator which makes the algorithm much more complex. Renewed interest in the modification of MAP decoding algorithm targeted in reduction of its

complexity without affecting its performance. The log-MAP and Max-Log-MAP algorithm substitute the MAP algorithm with the aid of the jacobian logarithm as defined in [49] by (3.10).

$$ln\left(\sum_{x_l}\exp\left(x_l\right)\right) = \begin{cases} \max_{x_l}\left\{x_l\right\} & \text{Max}-\text{Log}-\text{MAP} \\ \max_{x_l}^*\left\{x_l\right\} & \text{Log}-\text{MAP} \end{cases} \qquad (3.10)$$

Where max defines maximum operation. According to [17] the $\max^*(.)$ operation between x_1 and x_2 given by:

$$\overset{*}{\max}\left(x_1, x_2\right) = \max\left\{x_1, x_2\right\} + \underbrace{\ln\left(1 + \exp\left(-\left|x_1 - x_2\right|\right)\right)}_{\text{Correction term}}$$

The difference between Log-MAP and Max-Log-MAP algorithms lies in the way both treat the jacobian logarithm. The Log-MAP uses correction term in addition to the $\max(.)$ operation, whereas Max-Log-MAP uses the exact $\max(.)$ operation only. By utilizing Max-Log-MAP or log-MAP based soft values with interleaver type similar to the encoder interleaver turbo decoder estimates the original bit sequences iteratively. After the final iteration has been completed turbo decoder makes a hard decision to determine whether the transmitted bit is zero or one i.e.

$$L\left(x'_{l,t}/r\right) \overset{\overset{u'=1}{>}}{\underset{\underset{u'=0}{\leq}}{}} 0 \qquad (3.11)$$

If the last iteration of the second component decoder LLR value $L\left(x'_{l,t}/r\right)$ greater than zero it is favorable to decide bit being 1 else it decides to the bit being 0.

3.2.2.5 Turbo Trellis Code Termination

Conventional convolutional code uses a stream of zeros as tail bits to terminate the code depending on the state of the encoder after all data bits have been encoded. For turbo code due to the presence of interleaver between the two-component encoder, the final state among them will be different. Also, the trellis termination

bits differ in each component encoder and cannot attain zero states by appending steam of zeros like convolutional code. Therefore, turbo code terminates using a sequence of feedback bits to the encoder input as shown in Figure 3.6.
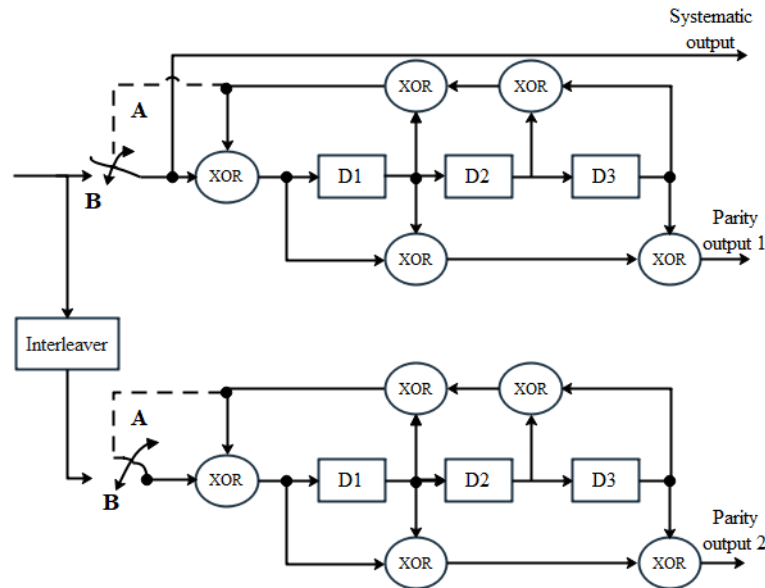
FIGURE 3.6: Trellis termination mechanism of turbo code.

At the ends of input data bit sequences are encoded the switch moves to position A to terminate the code trellis by generating tail bits automatically. The generating tail bits depend on the state and the encoded sequence.

In the iterative turbo decoding process, the BER of the decoded bits falls on average as the iteration increase. However, as additional iteration is carried out the improvement in BER performance has not that much significant. Therefore, for complexity reasons usually, only a certain number of iterations are carried out. In this thesis work, an iteration order with the convergence of BER performance gain has been used. Also, turbo code performance can further improve by increasing the constraint length with generator polynomials that have a large minimum free distance. However, a large constraint length introduces complexity and latency. As a result, in this study turbo code structure depicted in Figure 3.6 having a constraint length $K = 4$ with optimal performance of feedback $g_1 = 17_{(oct)}$ and feed forward $g_2 = 15_{(oct)}$ generator polynomials [40] has been used.

3.3   Space Time Block Code

Space time block coding is a powerful transmitter diversity technique that relies on the coding of the transmitted symbols across space and time to extract diversity. In STBC design of matrix G rows of the code matrix are orthogonal to each other, thus allows for simple recovery of the transmitted symbols without interfering with each other. The STBC encoder takes modulated symbols x and encodes them in a matrix form with rows of T time slots and columns of N_t transmit antennas given by (3.12) [40].

$$G_{N_t} = \begin{bmatrix} X_{1,1} & X_{1,2} & \dots & X_{1,N_t} \\ X_{2,1} & X_{2,2} & \dots & X_{2,N_t} \\ \vdots & \ddots & & \vdots \\ X_{T,1} & X_{T,2} & \dots & X_{T,N_t} \end{bmatrix} \tag{3.12}$$

The matrix G_{N_t} contains modulated symbols x and its conjugated version. In this thesis, Alamouti STBC having a transmitter antenna $N_t = 2$ and time slot $T = 2$ with the space-time codeword matrix (3.13) has been used.

$$G_2 = \begin{bmatrix} X_1 & X_2 \\ -X_2^* & X_1^* \end{bmatrix} \tag{3.13}$$

Where $*$ denotes complex conjugate operation. In the first time slot X_1 transmitted from the first antenna and X_2 transmitted from the second antenna. In second time slot $-X_2^*$ and X_1^* are transmitted from the first and second antenna respectively. In STBC the rate R_s is defined by the number of different symbols in each transmitter antenna divided by its time slot T.

3.4   OFDM and MIMO-OFDM System

3.4.1   OFDM System

In the OFDM modulation scheme, the available bandwidth divides into several narrow-band sub-carriers that are nearly flat fading. OFDM modulation is spectral efficient over conventional MCM. In conventional frequency division multiplexing (FDM) modulation, each sub-carrier transmits at different frequencies with enough spacing in between them. Due to the non-orthogonal nature of carrier frequencies in FDM, a large bandgap is required to avoid inter-channel interference, which reduces the overall spectral efficiency [50]. OFDM solves this bandwidth inefficiency using the orthogonal principle.

In orthogonality, the center of one sub-carrier is positioned into the null of the other neighboring sub-carrier as shown in figure 3.10b. Figure 3.7 illustrates the bandwidth saved by OFDM over the conventional multicarrier technique.
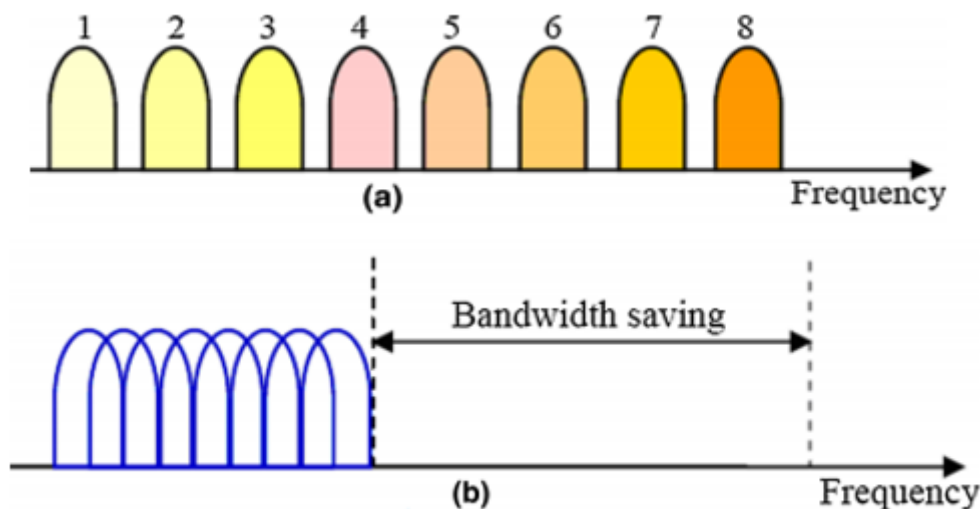
FIGURE 3.7: Spectral efficiency in conventional MCM (a) and orthogonal MCM (b) techniques [10].

The basic block diagram of the OFDM transceiver system has shown in Figure 3.8. In the transmitter, the N length parallel complex modulation symbol streams $X = [X(0),\, X(1),\dots,X(N-1)]^T$ undergo baseband OFDM modulation. Where $[.]^T$

denotes the transpose operation. This OFDM modulation has implemented using Inverse Fast Fourier Transform (IFFT) to obtain its time domain symbol.
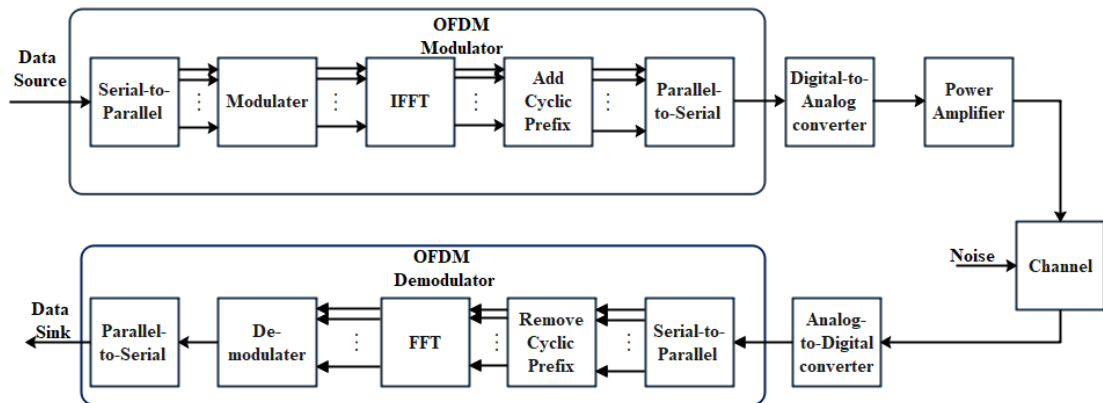
FIGURE 3.8: Block diagram of OFDM transceiver system.

Guard interval or cyclic prefix (CP), which is the copy of the last symbols of the transmitted data, shown in Figure 3.9, with a length larger than the delay spread of the channel added to the OFDM symbols. CP appended to each data symbol to prevent inter-symbol interference. The data are now sent to the receiver through the channel after it is amplified by the power amplifier. At the receiver, basically, the inverse of the transmitter process occurs.
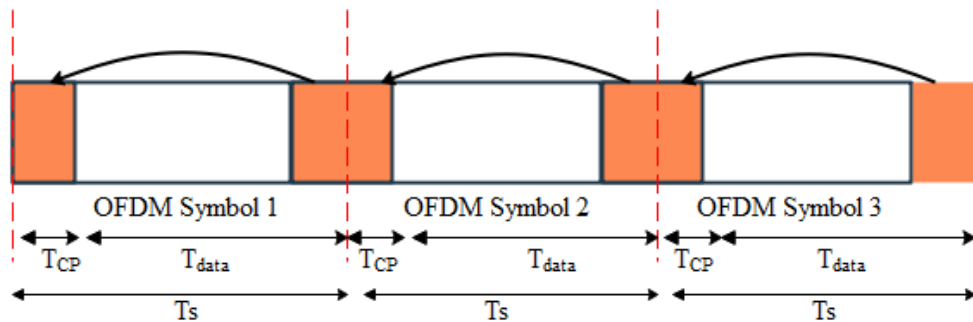
FIGURE 3.9: CP insertion mechanism in OFDM system.

The continuous-time baseband OFDM signal is defined as the sum of all N sub-carriers with sub-carrier spacing $f = \frac{1}{NT_s}$ in [10] given by:

$$x(t) = \sum_{k=0}^{N-1} X(k) e^{j2\pi \frac{k}{NT_s} t}, \quad 0 \leq t < NT_s \tag{3.14}$$

Where $X(k)$ denotes the OFDM frequency domain signal at k^{th} sub-carrier index and T_s is the OFDM symbol time interval given by the sum of data time duration T_{data} and CP time duration T_{CP} i.e.

$$T_s = T_{data} + T_{CP} \tag{3.15}$$

By sampling $x(t)$ at Nyquist rate $t = nT_s$ with $n = 0, 1, 2, \ldots, N-1$ the discrete time OFDM signal $x[n]$ can be express as [15]:

$$x[n] = \frac{1}{\sqrt{N}} \sum_{k=0}^{N-1} X(k) e^{j2\pi \frac{k}{N}n} \tag{3.16}$$

3.4.2 MIMO-OFDM System

The application of STBC to MIMO systems using OFDM modulation allows increasing system reliability through spatial diversity. Consider STBC MIMO-OFDM system having N_t transmitter antenna and N_r receiver antenna shown in Figure 3.10.
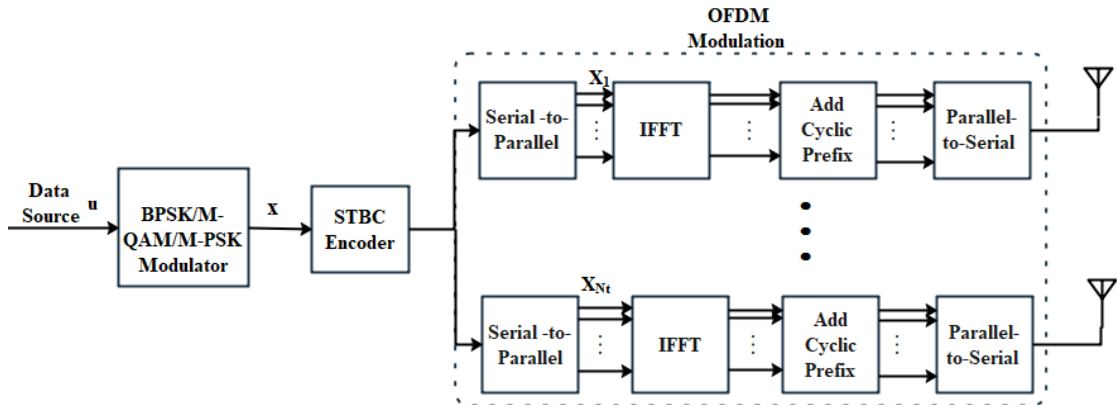
FIGURE 3.10: Block diagram of STBC MIMO-OFDM transmitter.

In the MIMO-OFDM system, the conventional OFDM modulation is employed at each transmitter antenna. Let's consider the N IFFT points from the ith transmitter antenna after serial-to-parallel conversion represent by the frequency domain signal $\{X_i[k]\}_{k=0}^{N-1}$. The corresponding discrete-time baseband OFDM signal $x_i[n]$

after applying IFFT is given as:

$$x_i[n] = \frac{1}{\sqrt{N}} \sum_{k=0}^{N-1} X_i[k] e^{j2\pi\frac{k}{N}n}, \quad n = 0, 1, \dots, N-1 \ \ i = 1, 2, \dots, N_t \quad (3.17)$$

Where k, n denotes the frequency index and the discrete time index respectively.

Assume the STBC MIMO-OFDM system consists of $N_t \times N_r$ independent channel coefficients h is given by:

$$h = \begin{bmatrix} h_{1,1} & h_{1,2} & h_{1,3} & \dots & h_{1,N_r} \\ h_{2,1} & h_{2,2} & h_{2,3} & \dots & h_{2,N_r} \\ \ddots & & & \dots & \ddots \\ h_{N_t,1} & h_{N_t,2} & h_{N_t,3} & \dots & h_{Nt,N_r} \end{bmatrix} \quad (3.18)$$

Where $h_{i,j}$ is a complex number that represents the channel gain between i^{th} transmitter antenna and j^{th} receiver antenna. For J number of paths the independent channel gain can be expressed using (3.19).

$$h_{i,j} = [h_{i,j}[0], \ h_{i,j}[1], \ h_{i,j}[2], \ \dots, h_{i,j}[J-1]]^T \quad (3.19)$$

The discrete channel response of sub-carriers between i^{th} transmitter antenna and j^{th} receiver antenna given by:

$$H_{i,j}[k] = \sum_{q=0}^{J-1} h_{i,j}[q] e^{-j2\pi\frac{q}{N}k} \quad (3.20)$$

Assume that there is perfect time synchronization and the cyclic prefix length greater than the path delay length J so that there is no inter-symbol interference between OFDM symbols. Now the received MIMO-OFDM data $R_j[k]$ shown in Figure 3.11 at the jth receiver antenna after OFDM demodulation applied can express in matrix form as [13]:

$$R_j[k] = \sum_{i=1}^{N_t} H_{i,j}[k] X_i[k] + W_j[k] \quad (3.21)$$

Where $W_j[k]$ represents the FFT of white Gaussian noise in the jth receive antenna with variance σ^2. Now let consider STBC MIMO-OFDM system having a transmitter antenna $N_t = 2$, the receiver antenna N_r and a time slot $T = 2$.
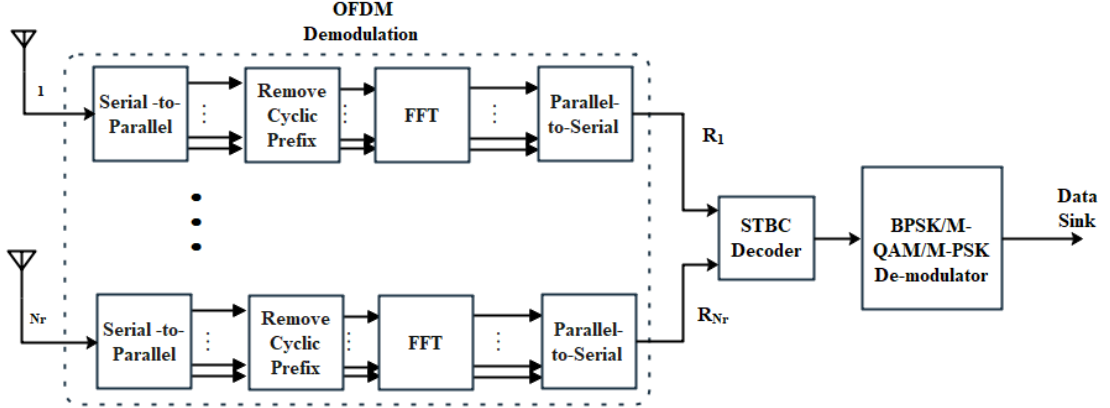
FIGURE 3.11: Block diagram of STBC MIMO-OFDM receiver.

To have sub-carrier length N at a given time slot each of the transmitter antennas fed with data having a length of $2N$. The STBC encoder output data symbols in equation (3.13) after serial to parallel conversion at time slot 1 and 2 given as:

$$
\begin{aligned}
X_{1,1} &= \begin{bmatrix} x_0 \ x_2 \ x_4 \ldots x_{2N-2} \end{bmatrix}^T &= X_1 \\
X_{1,2} &= \begin{bmatrix} x_1 \ x_3 \ x_5 \ldots x_{2N-1} \end{bmatrix}^T &= X_2 \\
X_{2,1} &= \begin{bmatrix} -x_1^* - x_3^* - x_5^* \ldots - x_{2N-1}^* \end{bmatrix}^T &= -X_2^* \\
X_{2,2} &= \begin{bmatrix} x_0^* \ x_2^* \ x_4^* \ldots x_{2N-2}^* \end{bmatrix}^T &= X_1^*
\end{aligned}
\tag{3.22}
$$

Where $X_{t,i}$ denotes the symbol stream in the transmitter antenna i at time slot t. Assume that the channel fading coefficient is constant over a time slot $T = 2$. Now using transmitting antennas $N_t = 2$ and receiving antennas N_r equation (3.21) give as:

$$
\begin{aligned}
R_{1,j}[k] &= \sum_{j=1}^{N_r} H_{1,j}[k] X_1[k] + H_{2,j}[k] X_2[k] + W_{1,j}[k] \\
R_{2,j}[k] &= \sum_{j=1}^{N_r} -H_{1,j}[k] X_2^*[k] + H_{2,j}[k] X_1^*[k] + W_{2,j}[k]
\end{aligned}
\tag{3.23}
$$

Where $R_{1,j}[k]$ and $R_{2,j}[k]$ denotes the received signal by receiving antenna j in sub-carrier index k at time slot 1 and 2 respectively. Having the knowledge of the channel at the receiver (in this thesis work perfect channel state information has

assumed) the STBC decoder recovers data symbols X'_1 and X'_2 using (3.24).

$$
\begin{aligned}
X'_1[k] &= \sum_{j=1}^{N_r} \left(H^*_{1,j}[k] R_{1,j}[k] + H_{2,j}[k] R^*_{2,j}[k] \right) \\
X'_2[k] &= \sum_{j=1}^{N_r} \left(H^*_{2,j}[k] R_{1,j}[k] - H_{1,j}[k] R^*_{2,j}[k] \right)
\end{aligned}
\tag{3.24}
$$

Both X'_1 and X'_2 are then passed to the maximum likelihood detector to determine the most likely transmitted symbol X'' based on the Euclidean distances between the STBC recovered signal and all possible transmitted symbol [40] i.e.

$$
\begin{aligned}
X''[2k-1] &= \min_{X_1} \left\{ \|X'_1[k] - X_1\|^2 + \left(\sum_{j=1}^{N_r} \sum_{i=1}^{2} \|H_{i,j}[k]\|^2 - 1 \right) \|X_1\|^2 \right\} \\
X''[2k] &= \min_{X_2} \left\{ \|X'_2[k] - X_2\|^2 + \left(\sum_{j=1}^{N_r} \sum_{i=1}^{2} \|H_{i,j}[k]\|^2 - 1 \right) \|X_2\|^2 \right\}
\end{aligned}
\tag{3.25}
$$

Where $k = 1, 2, \ldots, \text{N}$

3.5 PAPR in MIMO-OFDM System

As illustrated in the introduction section high PAPR is one limitation of OFDM as well as MIMO-OFDM system. This happens due to the existence of high peak envelope compared to the average envelope of the signal as shown in Figure 3.12.
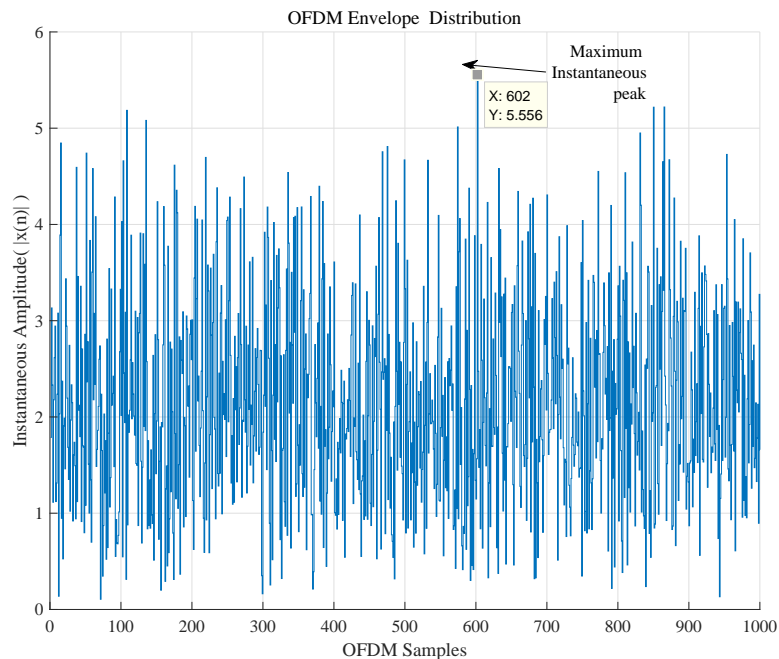
FIGURE 3.12: High peak envelope in OFDM signal generated by the addition of multiple sub-carriers.

PAPR is defined as the ratio of maximum instantaneous power to average power, within symbol duration. Mathematically PAPR of OFDM signal given by equation (3.26) [15], [18–20].

$$PAPR = \frac{\max\limits_{0 \leq t < NT_s} \left\{ \|x(t)\|^2 \right\}}{E\left[\|x(t)\|^2\right]} \tag{3.26}$$

Where $E[.]$ denotes the expectation operation. In most cases, the PAPR of the discrete OFDM signal is less than the PAPR of the continuous OFDM signal. Therefore, it is advisable to perform oversampling of the discrete OFDM signal to approximate the continuous-time PAPR [29][52]. After L-times interpolated $x[n]$ in (3.16) rewrite as:

$$x[n] = \frac{1}{\sqrt{LN}} \sum_{k=0}^{LN-1} \ddot{X}[k]\, e^{e^{j2\pi \frac{k}{NL} n}}, \quad 0 \leq n \leq NL - 1 \tag{3.27}$$

Where $\ddot{X}[k] = \begin{cases} X[k], & 0 \leq k < N/2 \ and \ NL - N/2 < k < NL \\ 0 & elsewhere \end{cases}$

The PAPR using this L oversampling discrete OFDM signal express by equation (3.28)[15].

$$PAPR = \frac{\max\limits_{0 \leq n \leq NL-1} \left\{ \|x[n]\|^2 \right\}}{E\left[\|x[n]\|^2\right]} \tag{3.28}$$

In dB equation (3.28) express as:

$$PAPR\,(dB) = 10\log_{10}\left(\frac{\max\limits_{0 \leq n \leq NL-1} \left\{ \|x[n]\|^2 \right\}}{E\left[\|x[n]\|^2\right]} \right) \tag{3.29}$$

Usually, $L \geq 4$ is used to accurately describe the PAPR of the continuous-time signal [52]. For MIMO-OFDM systems, the PAPR is defined as the maximum of all PAPR values evaluated among each transmitter antenna [29] i.e.

$$PAPR_{MIMO-OFDM} = \max\limits_{1 \leq i \leq N_t} \{PAPR_i\} \tag{3.30}$$

Where $PAPR_i$ is PAPR of OFDM signal from i^{th} transmitter antenna which has been evaluated using equation (3.28).

3.5.1 CCDF of PAPR

The CCDF of PAPR represents the probability that the peak to average power ratio exceeds a given threshold $PAPR_0$ i.e.

$$CCDF\left(PAPR\right) = pr\left(PAPR > PAPR_0\right) \tag{3.31}$$

CCDF is an important performance measure for evaluating the gain of PAPR reduction techniques. For independent and identically distributed data symbols the amplitude of OFDM complex signal samples $\{|x\left[n\right]|\}_{n=0}^{N-1}$ follows a Rayleigh distribution [51]. Using this assumption according to [38] equation (3.31) can approximate using (3.32).

$$CCDF\left(PAPR\right) = pr\left(PAPR > PAPR_0\right) \approx 1 - \left(1 - e^{-PAPR_0}\right)^N \tag{3.32}$$

The CCDF of N_t transmitter antenna MIMO-OFDM analog transmitted signal $x_i\left(t\right)$, which is actually amplified and transmitted, using its L-oversample discrete signal has been approximated by (3.33) [37].

$$CCDF\left(PAPR_{MIMO-OFDM}\right) = pr\left(PAPR_{MIMO-OFDM} > PAPR_0\right)$$
$$\approx 1 - \left(1 - e^{-PAPR_0}\right)^{NLN_t} \tag{3.33}$$

3.5.2 Effects of High PAPR in MIMO-OFDM System

Figure 3.13 illustrates the MIMO-OFDM system with the presence of HPA. Having the frequency domain signal $X_i\left[k\right]$ in the ith transmitter antenna the corresponding discrete-time baseband OFDM signal $x_i\left[n\right]$ after OFDM modulation has been computed using equation (3.17). Now let's consider the HPA transfer function in the linear and saturation regions shown in Figure 3.14. A highly fluctuating envelope signal with large a dynamic range in MIMO-OFDM system leads HPA to operate in the saturation region. This leads the amplified signal $S_i\left[n\right]$ subjected to non-linear distortion. To rideof the non-linear signal distortion, the HPA should

operate in its linear region at all power levels. This can be achieved using the input back-off (IBO). IBO of HPA in transmitter antenna i that delivers the desired linearity is defined as the ratio of its saturation power to the mean power of the input signal [3] i.e.

$$IBO_i\,(dB) = 10\log_{10}\left[\frac{P_{i\,sat}}{\left[E\,|x_i\,[n]|^2\right]}\right] \tag{3.34}$$

Where $P_{i\,sat}$ and $E\,|x_i\,[n]|^2$ denotes the saturation power level of HPA and the average power of the HPA input signal $x_i\,[n]$ in antenna i respectively.
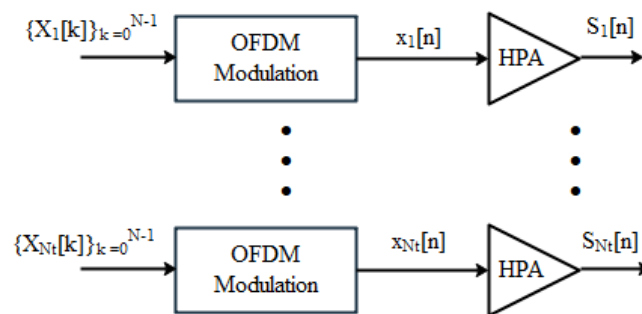
FIGURE 3.13: MIMO-OFDM transmission along with HPA.
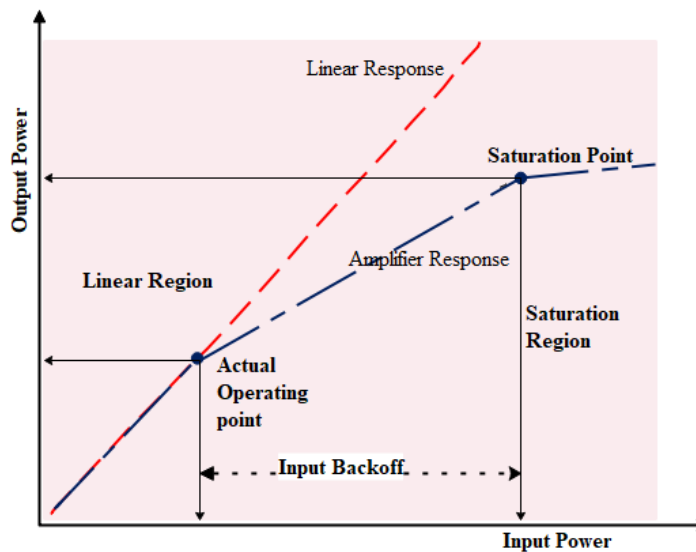
FIGURE 3.14: Transfer function of HPA.

High PAPR requires a large IBO which can be achieved by decreasing the mean power of the input signal thus resulting in poor power efficiency. For example, if we consider a class A amplifier, according to [52] its power efficiency is given by:

$$\eta = \frac{0.5}{PAPR} \times 100\% = \frac{0.5}{IBO} \times 100\% \,,\ IBO \geq 1 \tag{3.35}$$

The efficiency is inversely proportional to IBO and its maximum efficiency, (50%) occurs at IBO = 1 (0dB). Having poor power efficiency results in high energy consumption (low battery life) and short-range wireless communication. Therefore, to improve the amplifier efficiency without introducing non-linear distortion in the MIMO-OFDM system PAPR reduction techniques are required.

3.5.3 PAPR Reduction Techniques

The best alternative for reducing the high PAPR in the MIMO-OFDM system is to try to decrease the wide variations of the transmitted signal envelopes before the HPA. For this purpose, there are many proposed PAPR reduction techniques. Generally, PAPR reduction techniques can classify into four broad types as shown in Figure 3.15 [15]. Table 3.1 presents the advantages and disadvantages summary for each of the four general PAPR reduction techniques.
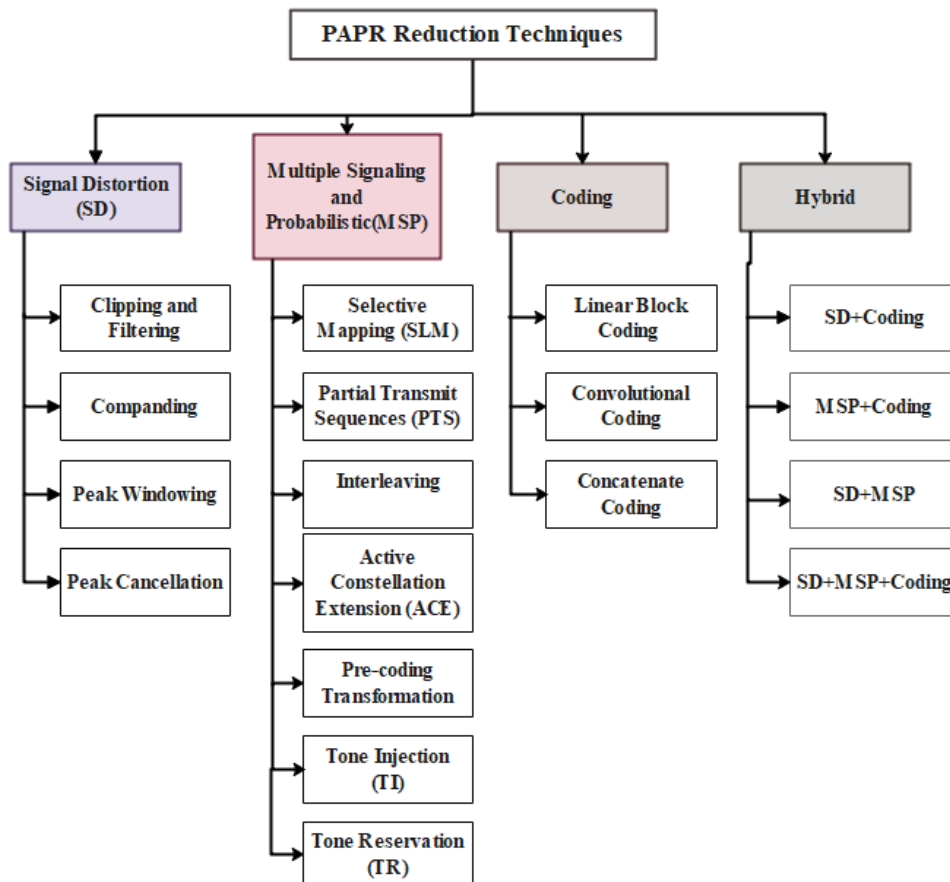
FIGURE 3.15: Categories of PAPR reduction techniques.

TABLE 3.1: Advantages and disadvantages of PAPR reduction techniques.

PAPR reduction techniques	Advantages	Disadvantages
SD	The most straightforward technique. Has yield relatively a better PAPR gain.	Introduces in-band and out-band distortion.
SMP	It does not introduce in-band and out-band distortion.	Spectral deficiency like in PTS, SLM. Complexity increases as subcarrier length increases (for example in SLM, PTS). Some of the techniques like pre-coding transformations have a comparatively small PAPR reduction ability.
Coding	It does not introduce in-band and out-band distortion. Enhance BER performance in addition to PAPR reduction.	Spectral deficiency due to additional overhead . Complexity to find out the best codeword with minimum PAPR value.
Hybrid	It has better PAPR reduction ability.	Relatively high complex. It introduces the drawbacks of each of the components of a hybrid technique.

Since the main intention of this thesis work relates to clipping-based PAPR reduction technique in section 3.5.3.1 the detail of clipping has been presented.

3.5.3.1 Clipping based PAPR Reduction in MIMO-OFDM System

Clipping is the simplest SD technique that reduces high PAPR in the MIMO-OFDM system by limiting the peak envelope of the OFDM modulated signal to the predefined threshold. The clipped signal $\overline{x}_i[n]$ with threshold A_{tr} has given by [23]:

$$\overline{x}_i[n] = \begin{cases} x_i[n], & |x_i[n]| < A_{tr} \\ A_{tr}e^{j\phi(x_i[n])}, & |x_i[n]| \geq A_{tr} \end{cases} \tag{3.36}$$

Where $x_i[n]$ is L-oversampled modulated OFDM signal in antenna i and $\phi(x_i[n])$ denotes its phase.

The value of A_{tr} is usually given as a function of clipping ratio γ and the ith transmitter antenna average signal power $P_i = E\|x_i[n]\|^2$ i.e.

$$A_{tr} = \gamma\sqrt{P_i} \tag{3.37}$$

By assuming each transmitter antenna has uniform average power i.e. $P_i = P$ and in terms of dB A_{tr} given as:

$$A_{tr} = 10^{(\gamma/20)} P \tag{3.38}$$

Although clipping can effectively reduce PAPR at a low threshold level, it introduces the following drawbacks [21–23]:

- In-band signal distortion thus results in BER performance degradation.

- Out-of-band radiation thus impose signal interference in the adjacent channels.

The out-of-band radiation in cclipping has already reduced by filtering but this introduces peak re-growth, so the peak envelopes after clipping and filtering could exceed the clipping threshold. To reduce overall peak re-growth, repeated clipping and filtering has used to obtain a desirable PAPR with increased computational complexity. In [53] a technique for the OFDM system has been proposed to reduce the computational complexity cost of repeated clipping and filtering.

Although filtering mitigates the out-of-band radiation it does not have any contribution for the reduction of in-band distortion. As the result, in-band distortion in clipping PAPR reduction technique has still an existing problem. Especially when the diversity order of MIMO-OFDM system has increased the BER deteriorates severely. Therefore, in chapter 4 a modified clipping technique with the application of powerful channel code (i.e turbo code) has been proposed to mitigate the BER performance degradation of the clipping-based MIMO-OFDM system.

Chapter 4

Proposed System Model

In this chapter, the overall proposed system model has been presented. In the first subsection, the design of modified clipping technique for high PAPR reduction of MIMO-OFDM system has presented. To compromise BER and PAPR performance trade-off in a better way turbo code has been applied. Since turbo decoder uses bit-wise soft information as input a Log-MAP based STBC detection has been presented in the second subsection of the chapter. In the final subsection, the proposed system computational complexity has been analyzed. Figure 4.1 shows shows the proposed turbo code based modified clipping MIMO-OFDM system.
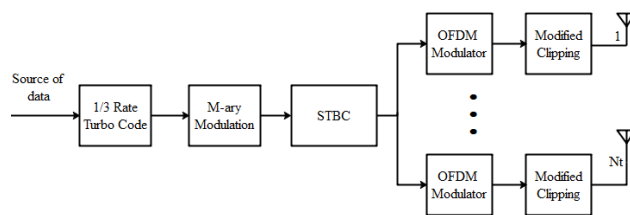
(a) Transmitter
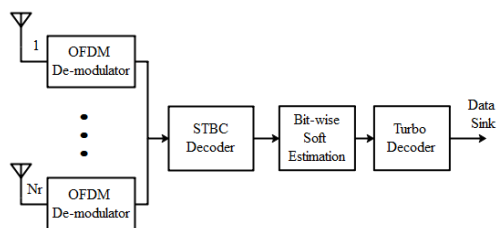
(b) Receiver

FIGURE 4.1: Proposed modified clipping MIMO-OFDM system with TC.

4.1 Modified Clipping Based PAPR Reduction

The main concern of modified clipping in the MIMO-OFDM system is to achieve a comparable PAPR reduction gain and better BER performance as compared to the conventional clipping MIMO-OFDM system. In modified clipping, the selected high peak envelopes have been clipped in successive manners rather than hard clipping like that of conventional clipping. Let's consider the L-oversampled OFDM signal in transmitter antenna i given by [51]:

$$x_i[n] = \frac{1}{\sqrt{NL}} \sum_{k=0}^{NL-1} \ddot{X}_i[k] e^{j2\pi \frac{k}{NL} n} \qquad (4.1)$$

Where $\ddot{X}_i$ is the L oversampled frequency domain OFDM signal in the ith antenna. In the design of the modified clipping technique, the first step is to find out O numbers of successive high peak envelopes from $x_i[n]$. This has been determined by sorting the instantaneous envelopes in ascending order and selecting O portions of the high peak envelopes i.e.

$$P_{i,1}[n] = \max\{|x_i[n]|\}$$
$$P_{i,2}[n] = \max\{|x_i[n]|\}, |x_i[n]| \notin \{P_{i,1}[n]\}$$
$$P_{i,3}[n] = \max\{|x_i[n]|\}, |x_i[n]| \notin \{P_{i,1}[n], P_{i,2}[n]\} \qquad (4.2)$$
$$\vdots \qquad \vdots$$
$$P_{i,O}[n] = \max\{|x_i[n]|\}, |x_i[n]| \notin \{P_{i,1}[n], P_{i,2}[n], \dots, P_{i,O-1}[n]\}$$

Where $P_{i,o}[.]$ is the successive high peak envelopes in the ith antenna such that $P_{i,1}[n] > P_{i,2}[n] > \dots > P_{i,O}[n]$. The next step in modified clipping design is grouping of the O number of successive peak envelopes into S number of quantization levels $Q_{i,1}[n], Q_{i,2}[n], Q_{i,3}[n], \dots, Q_{i,S}[n]$ in such a way that the difference between maximum to minimum peak envelope in each quantization level preserve to be constant i.e.

$$\Delta = \max\{Q_{i,m'}[n]\} - \min\{Q_{i,m'}[n]\} , \ m' = 1, 2, 3, \dots, S \qquad (4.3)$$

Where Δ denotes uniform step size used to set the selected high peak envelopes into one of the S numbers of quantization levels. Normally for the S number of quantization levels, there are $S - 1$ number of step sizes. Since for $m' = 2, 3, ..., S$ $\min(Q_{i,m'}[n]) = \max(Q_{i,m'-1}[n])$ (4.3) can rewrite as:

$$\Delta = \max(Q_{i,m'}[n]) - \max(Q_{i,m'-1}[n]), \, m' = 2, 3, ..., S \tag{4.4}$$

Another important parameter in modified clipping is the reduction level $RL_{i,m'}[n]$ of each peak envelope for each quantization level. The $RL_{i,m'}$ has evaluated using (4.5).

$$RL_{i,m'}[n] = \frac{\min\{Q_{i,m'}[n]\}}{Q_{i,m'}[n]} \tag{4.5}$$

Finally, the modified clipping MIMO-OFDM signal can express as:

$$\overline{x}_i[n] = \begin{cases} x_i[n], & |x_i[n]| < \min\{Q_{i,1}[n]\} \\ x_i[n] RL_{i,1}[n], & \min\{Q_{i,1}[n]\} \leq |x_i[n]| < \max\{Q_{i,1}[n]\} \\ x_i[n] RL_{i,2}[n], & \max\{Q_{i,1}[n]\} \leq |x_i[n]| < \max\{Q_{i,2}[n]\} \\ \vdots & \vdots \\ x_i[n] RL_{i,S}[n], & |x_i[n]| \geq \max\{Q_{i,S}[n]\} \end{cases} \tag{4.6}$$

Using the modified clipping signal $\overline{x}_i[n]$ the PAPR reduction has been evaluated as:

$$PAPR_i(dB) = 10\log_{10}\left(\frac{\max\limits_{0 \leq n \leq NL-1}\left\{\|\overline{x}_i[n]\|^2\right\}}{E\left[\|\overline{x}_i[n]\|^2\right]}\right) \tag{4.7}$$

The overall PAPR of the MIMO-OFDM system with N_t transmitter antenna has evaluated by

$$PAPR_{MIMO-OFDM} = \max\limits_{1 \leq i \leq N_t}\{PAPR_i(dB)\} \tag{4.8}$$

The number of quantization levels, step size value, and number of selected high peak envelopes are the factors of PAPR reduction in the modified clipping MIMO-OFDM system. In this thesis, the effects of one parameter have been evaluated by setting the other two parameters with fixed values. The Δ value decreases the selected peak envelope with a given quantization level has more chance to deeply clipped, thus reduces PAPR of MIMO-OFDM system. On the other hand, as the

numbers of quantization levels increase the signals with high peak envelope are less probable to deeply clip, and this results in relatively low PAPR reduction gain. Obviously, the PAPR reduction gain has directly proportional to the number of selected high peak envelopes.

4.2 Log-MAP STBC Detection and BER

Since the turbo decoder needs bit-wise soft information, a Log-MAP based bit-wise STBC detection has been adopted in this thesis work. The a posteriori probability $pr\left(X_v/R_j\right)$ of the transmitted symbol X_v ($v = 1,\ 2,\ ...\ , V$) allows for MAP based symbol-by-symbol STBC detection. For simplicity, by dropping the sub-carrier index k the $pr\left(X_v/R_j\right)$ has given in (4.9) [40].

$$pr\left(X_v/R_j\right) = pr\left(R_j/X_v\right).pr\left(X_v\right) \tag{4.9}$$

Where $\{R_j\}_{j=1}^{N_r}$ is the received signal in receiver antenna j which is given by (3.23), V denotes the number of symbols transmitted in a given transmitted antenna at time slot T and $pr\left(X_v\right)$ is a-priori information of the transmitted symbol X_v. The conditional pdf $pr\left(R_j/X_v\right)$ in [48] express as:

$$pr\left(R_j/X_v\right) = \frac{1}{\left(\sqrt{2\pi\sigma^2}\right)^{TN_r}} \exp\left(-\frac{1}{2\sigma^2}\sum_{j=1}^{N_r}\sum_{t=1}^{T}\left\|R_{t,j} - \sum_{i=1}^{N_t}X_{t,i}H_{i,j}\right\|^2\right) \tag{4.10}$$

Where $X_{t,i}$ represents the transmitted symbols or its conjugated version in time slot t and i^{th} transmitter antenna as given in (3.12). $H_{i,j}$ is the channel state information in i^{th} transmitter antenna and j^{th} receiver antenna (in this thesis perfect channel state information has been assumed). Having code rate R, average power P_{av} and m number of bits per transmitted symbol the noise variance σ^2 in (4.10) given by (4.11).

$$\sigma^2 = \frac{P_{av}}{R.m\left(E_b/N_0\right)} \tag{4.11}$$

Now for $N_t = 2$ and the associated time slot $T = 2$, $pr\left(R_j/X_v\right)$ express as:

$$pr\left(R_j/X_1,\ X_2\right) = \frac{1}{\left(\sqrt{2\pi\sigma^2}\right)^{2Nr}} \exp\left(-\frac{1}{2\sigma^2}\sum_{j=1}^{N_r}\sum_{t=1}^{2}\left\|R_{t,j} - \sum_{i=1}^{2}X_{t,i}H_{i,j}\right\|^2\right)$$
(4.12)

Using entries $X_{t,i}$ of G_2 from equation (3.13) $pr\left(R_j/X_1,\ X_2\right)$ further expand as:

$$pr\left(R_j/X_1,\ X_2\right) = C.\exp\left(-\frac{1}{2\sigma^2}\sum_{j=1}^{N_r}\left[\begin{array}{c}\|R_{1,j} - X_1H_{1,j} - X_2H_{2,j}\|^2 + \\ \|R_{2,j} + X_2^*H_{1,j} - X_1^*H_{2,j}\|^2\end{array}\right]\right)$$
(4.13)

Where $C = \frac{1}{\left(\sqrt{2\pi\sigma^2}\right)^{2Nr}}$. $X_1, X_2, X_1^*, -X_2^*$ denotes the N length column-wise STBC encoder output matrices defined by (3.22). Now using (4.13) the a posteriori probability $pr\left(X_v/R_j\right)$ in (4.9) becomes:

$$pr\left(X_v/R_j\right) = pr\left(X_1,\ X_2/R_j\right) = pr\left(R_j/X_1,\ X_2\right)pr\left(X_1,\ X_2\right)$$
$$= C.\exp\left(-\frac{1}{2\sigma^2}\sum_{j=1}^{N_r}\left[\begin{array}{c}\|R_{1,j} - X_1H_{1,j} - X_2H_{2,j}\|^2 + \\ \|R_{2,j} + X_2^*H_{1,j} - X_1^*H_{2,j}\|^2\end{array}\right]\right)pr\left(X_1,\ X_2\right)$$
(4.14)

Using the orthogonality property of the space-time block code matrix G_2 the expression in (4.14) can be decoupled for each symbol X_1 and X_2 as follows:

$$pr\left(X_1/R_j\right) = C.\exp\left(-\frac{1}{2\sigma^2}\sum_{j=1}^{N_r}\left[\|R_{1,j} - X_1H_{1,j}\|^2 + \|R_{2,j} - X_1^*H_{2,j}\|^2\right]\right)$$
$$pr\left(X_1\right)$$
(4.15)

$$pr\left(X_2/R_j\right) = C.\exp\left(-\frac{1}{2\sigma^2}\sum_{j=1}^{N_r}\left[\|R_{1,j} - X_2H_{2,j}\|^2 + \|R_{2,j} + X_2^*H_{1,j}\|^2\right]\right)$$
$$pr\left(X_2\right)$$
(4.16)

By eliminating codeword X_1 and X_2 independent terms and completing the square (4.15) and (4.16) rewritten as (4.17) and (4.18) respectively.

$$pr\left(X_1/R_j\right) = C.\exp\left(-\frac{1}{2\sigma^2}\left[\begin{array}{c}\left\|\left\{\sum_{j=1}^{N_r}\left(R_{1,j}H_{1,j}^* + R_{2,j}^*H_{2,j}\right)\right\} - X_1\right\|^2 \\ +\left(-1 + \sum_{j=1}^{N_r}\sum_{i=1}^{2}\|H_{i,j}\|^2\right)\|X_1\|^2\end{array}\right]\right)pr\left(X_1\right)$$
(4.17)

$$pr\left(X_2/R_j\right) = C.\exp\left(-\frac{1}{2\sigma^2}\left[\begin{array}{l}\left\|\left\{\sum_{j=1}^{N_r}\left(R_{1,j}H_{2,j}^* - R_{2,j}^*H_{1,j}\right)\right\} - X_2\right\|^2 \\ + \left(-1 + \sum_{j=1}^{N_r}\sum_{i=1}^{2}\|H_{i,j}\|^2\right)\|X_2\|^2\end{array}\right]\right)pr\left(X_2\right)$$

(4.18)

Normally the transmitted symbol X_1 and X_2 compose from the M-ary complex constellation symbols X. Assume there is no a-priori information i.e. all symbols to be equally likely and by assigning $pr\left(X_1/R_j\right)$ and $pr\left(X_2/R_j\right)$ to an odd and even sub-carrier index respectively equation (4.17) and (4.18) express by:

$$pr\left(X/R_j\right) = C.\exp\left(-\frac{1}{2\sigma^2}\left[\|R' - X\|^2 + H'\|X\|^2\right]\right)$$

(4.19)

Where

$$R'\left[2k - 1\right] = \sum_{j=1}^{N_r}\left(R_{1,j}\left[k\right]H_{1,j}^*\left[k\right] + R_{2,j}^*\left[k\right]H_{2,j}\left[k\right]\right)$$
$$R'\left[2k\right] = \sum_{j=1}^{N_r}\left(R_{1,j}\left[k\right]H_{2,j}^*\left[k\right] - R_{2,j}^*\left[k\right]H_{1,j}\left[k\right]\right)$$
$$H'\left[2k - 1\right] = H'\left[2k\right] = \left(-1 + \sum_{j=1}^{N_r}\sum_{i=1}^{2}\|H_{i,j}\left[k\right]\|^2\right)$$

Using (4.19) the bit-wise MAP soft information can estimate as shown below.

$$\begin{array}{l}L\left(u_l = 0\right) = \sum pr\left(X/R_j\right), \quad \forall X = \left(u_1 \ \ldots \ u_l \ \ldots u_m\right), \quad u_l = 0 \\ L\left(u_l = 1\right) = \sum pr\left(X/R_j\right), \quad \forall X = \left(u_1 \ \ldots \ u_l \ \ldots \ u_m\right), \quad u_l = 1\end{array}$$

(4.20)

Where $u = [u_1, u_2 \ldots \ u_m]$ is the m-tuple bit sequence corresponding to the symbol X. Using the above bit-wise MAP soft information the LLR of the lth bit $L\left(u_l\right)$ can express as:

$$L\left(u_l\right) = \ln\left(\frac{\sum_{\forall X_l \Rightarrow 1} pr\left(X_l/R_j\right)}{\sum_{\forall X_l \Rightarrow 0} pr\left(X_l/R_j\right)}\right)$$

(4.21)

Although MAP based detection has optimal performance it has high computational complexity [17]. Therefore, a sub-optimal Log-MAP based STBC detection has been used in this thesis work. Using Log-MAP detection equation (4.21) express as:

$$L\left(u_l\right) = \max_{\forall X_l = 1}^{*}\left(pr\left(X/R_j\right)\right) - \max_{\forall X_l = 0}^{*}\left(pr\left(X/R_j\right)\right)$$

(4.22)

Where Log-MAP between x_1 and x_2 defined by (4.23) [17],[40].

$$
\begin{aligned}
\max{}^* (x_1, x_2) &= \ln \left(\exp \left(x_1 \right) + \exp \left(x_2 \right) \right) \\
&= \max \left\{ x_1, x_2 \right\} + \underbrace{\ln \left(1 + \exp \left(- \left| x_1 - x_2 \right| \right) \right)}_{\text{Correction term}}
\end{aligned}
\tag{4.23}
$$

Where $max \left(. \right)$ is a maximum operator. The correction term in Log-MAP need not be computed for every received sequence instead it can be stored in a look-up table [40], [55]. Using the Log-MAP soft bit-wise information as input an iterative estimation in between each component turbo decoder has been performed to recover the transmitted data sequences. Consider u'_k as the estimated information bit at time k, and in the s' starting state and s ending state of the trellis section.

According to [40] the LLR of the estimated information bit u'_k at time k in each turbo decoder using Log-MAP algorithm express as:

$$
\begin{aligned}
L \left(u'_k \right) = {}& \max_{(s',s) \Rightarrow u_k \Rightarrow 1}{}^* \left(A_{k-1} \left(s' \right) + \Gamma_k \left(s', s \right) + B_k \left(s \right) \right) \\
& - \max_{(s',s) \Rightarrow u_k \Rightarrow 0}{}^* \left(A_{k-1} \left(s' \right) + \Gamma_k \left(s', s \right) + B_k \left(s \right) \right)
\end{aligned}
\tag{4.24}
$$

Where $A_k \left(s \right)$, $B_{k-1} \left(s' \right)$, and $\Gamma_k \left(s', s \right)$ denote the forward recursion, backward recursion, and branch metrics. The full derivation of $L \left(u'_k \right)$ has illustrated in the appendix. For rate $\frac{1}{n}$ the forward recursion, backward recursion, and branch metrics are given by (4.25), (4.26), and (4.27).

$$
\begin{aligned}
A_k \left(s \right) &= \ln \left(\sum_{\forall s'} \exp \left(A_{k-1} \left(s' \right) + \Gamma_k \left(s', s \right) \right) \right) \\
&= \max_{\forall s'}{}^* \left(A_{k-1} \left(s' \right) + \Gamma_k \left(s', s \right) \right)
\end{aligned}
\tag{4.25}
$$

$$
\begin{aligned}
B_{k-1} \left(s' \right) &= \ln \left(\sum_{\forall s} \exp \left(B_k \left(s \right) + \Gamma_k \left(s', s \right) \right) \right) \\
&= \max_{\forall s}{}^* \left(B_k \left(s \right) + \Gamma_k \left(s', s \right) \right)
\end{aligned}
\tag{4.26}
$$

.

$$
\Gamma_k \left(s', s \right) = \sum_{z=1}^{n} x'_{z,k} . x_{z,k} \left(s', s \right) + La_k . u_k \left(s', s \right)
\tag{4.27}
$$

Where $x_{z,k} \left(s', s \right)$ and $u_k \left(s', s \right)$ denotes the zth bits of the codeword and the information bit respectively associated with the state branch $\left(s', s \right)$. La_k is the

priori value from the component turbo decoder and $x'_{z,k}$ is the zth noisy bit-wise soft information for the codeword $x_{z,k}$ which is has been already obtained from (4.22). After the final iteration is being completed, the proposed TC-based modified clipping MIMO-OFDM communication links quality has evaluated using BER performance metrics.

The BER of the proposed system at a time is given by the absolute value of the difference between the original transmitted bit sequence and the TC hard decision received bit sequence. For the overall received bit sequences, the BER calculate by:

$$BER = \frac{\text{Total number of errors}}{\text{Total number of transmitted bits}} \tag{4.28}$$

The designed modified clipping parameters relate with BER performance in the opposite manner to the PAPR reduction gain. The number of selected peak envelopes has a direct impact on the transmitted signal distortion. On the other hand, the transmitted signal distortion inversely relates to the number of quantization levels and the step size value. Meanwhile, the BER performance and the signal distortion are inversely related to each other.

Further apart from the parameters of modified clipping the proposed system BER performance depends on turbo decoder algorithm type, the constraint length, the generator polynomial connection, the number of turbo decoder iterations, turbo interleaver type, and MIMO diversity order. For complexity reason Log-MAP decoder having constraint length (K) four and random interleaver type with suboptimal performance feedback $g_1 = 17_{(oct)}$ and feedforward $g_2 = 15_{(oct)}$ generator polynomial connection [40] has been used in this thesis work.

4.3   System Complexity Analysis

In this subsection, the complexity of the proposed system has been illustrated. The computational complexity analysis has been done for the transmitter and receiver parts separately. To simplify the computational complexity analysis the receiver of

the proposed system again divides into three parts: OFDM demodulation in each receiver antenna, Log-MAP based STBC detection and Log-MAP based turbo decoding. The proposed system's computational complexity has been compared with the respective computational complexities of the conventional clipping, a hybrid partial transmit sequence proposed in [33], and a low complexity selective mapping technique demonstrated in [31].

In both the transmitter and the receiver of the proposed system, the computational complexity has been estimated in terms of real multiplication/division (MUL) and real addition/subtraction (ADD). In addition to MUL and ADD the Log-MAP-based STBC detection and turbo decoding complexity have been calculated in terms of $max(.)$ operations and look-up tables. For real MUL and real ADD analysis, let's consider the multiplication and addition between two complex terms a and b i.e.

$$(a_\Re + ja_\Im)(b_\Re + jb_\Im) = (a_\Re b_\Re - a_\Im b_\Im) + j(a_\Re b_\Im + a_\Im b_\Re)$$

This needs 4 real MULs and 2 real ADDs.

$$(a_\Re + ja_\Im) + (b_\Re + jb_\Im) = (a_\Re + b_\Re) + j(a_\Im + b_\Im)$$

This needs 2 real ADDs.

With N point FFT/IFFT the computation of OFDM in each transmitter antenna has required $C_{OFDM}^{T_x}$ real multiplication and $A_{OFDM}^{T_x}$ real addition [54].

$$C_{OFDM}^{T_x} = N\left(\log_2^N - 3\right) + 4 \tag{4.29}$$

$$A_{OFDM}^{T_x} = 3N\left(\log_2^N - 1\right) + 4 \tag{4.30}$$

Therefore, using L oversampling the LN-points FFT operation in each transmitter antenna requires $LN\left(\log_2^{NL} - 3\right) + 4$ real MULs and $3LN\left(\log_2^{LN} - 1\right) + 4$ real ADDs. The determination of $|x[n]|$ needs additional $2LN$ real MULs and LN real ADDs in each transmitter antenna. For a given clipping ratio value, the calculation of its corresponding threshold value in conventional clipping using (3.37) needs 2 real MULs (i.e. 1 real multiplication and 1 division) and LN real ADDs per transmitter antenna. On the other hand, the designed modified clipping is independent of the clipping threshold level and for O clipped envelopes with S

quantization levels the designed modified clipping evaluation in (4.6) requires $2O$ real MULs and $S - 2$ real ADDs per a transmitter antenna.

The proposed hybrid PTS based PAPR reduction technique in [33] with V is sub-block sequences requires $\frac{N}{4}\left(log_2\frac{N}{V} + Vlog_2N + 2V\right)$ complex multiplications and $\frac{N}{2}\left(log_2\frac{N}{V} + Vlog_2N\right)$ complex additions along each transmitter antenna. Therefore, the computation of the proposed hybrid PTS work in [33] for each transmitter antenna using L oversample takes $NL\left(log_2\frac{LN}{V} + Vlog_2LN + 2V\right)$ real MULs and $NL\left(\frac{3}{2}log_2\frac{LN}{V} + \frac{3}{2}Vlog_2LN + V\right)$ real ADDs. Further apart from this, the proposed modified clipping complexity compare to the low complexity extended SLM-based PAPR reduction work conducted in [31]. For the proposed work its computation with V sub-blocks, C contiguous extended sub-blocks, and E basic data unit sub-blocks in each transmitter antenna needs $NLlog_2\frac{LN}{2C} + 2LN\left(2C + EV\right)$ complex multiplications and $2NLlog_2\frac{LN}{2C} + LNV\left(4C - 2\right)$ complex additions. As a result, in [31] the total required real multiplications and real additions per transmitter antenna becomes $4\left(NLlog_2\frac{LN}{2C} + 2LN\left(2C + EV\right)\right)$ and $6NLlog_2\frac{LN}{2C} + 4LNV\left(2C + \frac{2C}{V} + E - 1\right)$, respectively.

The overall transmitter side computational complexity of the designed modified clipping, conventional clipping, hybrid PTS in [33], and SLM in [31] for MIMO-OFDM system with N_t transmitter antennas have been summarized in Table 4.1.

TABLE 4.1: The computational complexity of proposed modified clipping, conventional clipping, PTS [33], and SLM [31] for the MIMO-OFDM transmitter side.

PAPR reduction method	Real multiplication / division	Real addition/ subtraction
Proposed modified clipping	$N_t\left(LN\left(log_2^{NL} - 3\right) + 2LN + 2O + 4\right)$	$N_t\left(3LN\left(log_2^{LN} - 1\right) + LN + S + 2\right)$
Conventional clipping	$N_t\left(LN\left(log_2^{NL} - 3\right) + 2LN + 6\right)$	$N_t\left(3LN\left(log_2^{LN} - 1\right) + 2LN + 4\right)$
Hybrid PTS [33]	$NLN_t\left(log_2\frac{LN}{V} + Vlog_2LN + 2V\right)$	$NLN_t\left(\frac{3}{2}log_2\frac{LN}{V} + \frac{3}{2}Vlog_2LN + V\right)$
SLM without SI [31]	$4N_t\left(NLlog_2\frac{LN}{2C} + 2LN\left(2C + EV\right)\right)$	$N_t\left(6NLlog_2\frac{LN}{2C} + 4LNV\left(2C + \frac{2C}{V} + E - 1\right)\right)$

To start the receiver complexity estimation of the proposed system let's consider the first subsystem i.e. OFDM demodulation complexity analysis. Using (4.29) and (4.30) with L oversampling and N_r receiver antennas the OFDM demodulation

requires $N_r \left(LN \left(\log_2^{NL} - 3 \right) + 4 \right)$ real MULs and $N_r \left(3LN \left(\log_2^{LN} - 1 \right) + 4 \right)$ real ADDs.

In Log-MAP STBC detection complexity analysis, each term in (4.22) has been considered. The computation of R' in (4.19) for each received signal needs $4N_t.N_r$ real MULs and $2N_t.N_r$ real ADDs (from complex multiplication). Also, $N_t.N_r - 1$ complex additions of R' result in $2 \left(N_t.N_r - 1 \right)$ real ADDs for each received signal. Additionally, 2 real MULs and 5 real ADDs needs for the computation of $\| R' - X \|^2 = \left[\Re \left(R' - X \right) \right]^2 + \left[\Im \left(R' - X \right) \right]^2$ in each received signal. Where $\Re \left(. \right)$ and $\Im \left(. \right)$ are the real and imaginary parts of a complex-valued quantity. H' in (4.19) can rewrite as:

$$H' = \left(-1 + \sum_{j=1}^{N_r} \sum_{i=1}^{N_t} \| H_{i,j} \|^2 \right) = -1 + \sum_{j=1}^{N_r} \sum_{i=1}^{N_t} \left[\Re \left(H_{i,j} \right) \right]^2 + \left[\Im \left(H_{i,j} \right) \right]^2$$

As a result, H' takes $2N_t.N_r$ real MULs and $2N_t.N_r$ real ADDs at a time. Similarly, $\| X \|^2$ needs 2 real MULs and 1 real ADDs per symbol. Also, one real ADD and two real MULs needs for $-\frac{1}{2\sigma^2} \left(\| R' - X \|^2 + H' \| X \|^2 \right)$ computation . Finally, in max^* operation of (4.22) one real ADD has been needed.

Note that in the lth bit-wise estimation the computation requirement of real MULs and real ADDs in $\| R' - X \|^2$, $\| X \|^2$, $H' \| X \|^2$, and $-\frac{1}{2\sigma^2} \left(\| R' - X \|^2 + H' \| X \|^2 \right)$ increase by a factor of 2^m. Where $l = 1, 2, \ldots, m$ and m is the number of bits in the M-ary complex symbol. After OFDM demodulation and L down-sampled in STBC detection a total $N.N_t$ signals have been received. Therefore, the computation of $-\frac{1}{2\sigma^2} \left[\| R' - X \|^2 + H' \| X \|^2 \right]$ with m bits and $N.N_t$ received signals needs $C_{Log-MAP}^{STBC}$ real MULs and $A_{Log-MAP}^{STBC}$ real ADDs.

$$C_{Log-MAP}^{STBC} = N.N_t \left(6m.2^m + 6N_t N_r \right) \tag{4.31}$$

$$A_{Log-MAP}^{STBC} = N.N_t \left(m \left(1 + 7.2^m \right) + 6N_t N_r - 2 \right) \tag{4.32}$$

Rather than the direct computation of correction term in the Log-MAP algorithm for this thesis work look-up table has been suggested [40], [55]. One max^* operation

works on two input terms. Also, one max^* needs one $max\,(.)$ and one look-up table for a single bit-wise estimation. As a result, for m bits and $N.N_t$ received signals (4.22) requires $Max_{Log-MAP}^{STBC}$ max operations and $Lt_{Log-MAP}^{STBC}$ look-up tables.

$$Max_{Log-MAP}^{STBC} = 2mN.N_t \left(2^{m-1} - 1\right) \tag{4.33}$$

$$Lt_{Log-MAP}^{STBC} = 2mN.N_t \left(2^{m-1} - 1\right) \tag{4.34}$$

In uncoded MIMO-OFDM system, the symbol maximum likelihood based STBC detection has been held using (3.25). As a result, in ML STBC detection the real ADDs and MULs requirements are not proportional to m rather they proportional to the 2^m M-ary modulation order. Also, the multiplication with $-\frac{1}{2\sigma^2}$ has not been required. Therefore, the ML based symbol STBC detection needs C_{ML}^{STBC} real MULs and A_{ML}^{STBC} real ADDs.

$$C_{ML}^{STBC} = N.N_t \left(5.2^m + 6N_tN_r\right) \tag{4.35}$$

$$A_{ML}^{STBC} = N.N_t \left(7.2^m + 6N_tN_r - 2\right) \tag{4.36}$$

Unlike Log-MAP based STBC detection the ML based STBC detection did not require look-up tables for correction terms. Therefore, ML based STBC detection has needed Max_{ML}^{STBC} max operation.

$$Max_{ML}^{STBC} = N.N_t \left(2^m\right) \tag{4.37}$$

The remaining part in the complexity analysis of the proposed system is the Log-MAP based turbo decoding complexity. The analysis of Log-MAP-based turbo decoding complexity has been done using $A_k\,(s)$, $\Gamma_k\,(s', s)$, and $B_{k-1}\,(s')$ metrics. Basically, interleaver size, constraint length (K), numbers of constitute decoders, and the number of decoder iterations are factors that influence the complexity of Log-MAP-based turbo decoding.

For $\frac{1}{n}$ rate and 2^{K-1} total states the computation of the codeword correlation between $x'_{z,k}$ and $x_{z,k}\,(s', s)$ for branch metric in (4.27) has required $2^K n$ MULs

and $2^K (n-1)$ ADDs per a systematic bit [55]. The computation of information bit u_k in the branch (s', s) with a-priori value requires 2^K MULs. Additionally, 2^K ADDs need to be added $La_k.u_k(s', s)$ with codeword correlation. Therefore, the computation of $\Gamma_k(s', s)$ per a systematic bit needs $2^K(n+1)$ real MULs and $2^K(n)$ real ADDs [55]. The computation of the forward recursion given in (4.25) needs 2^K real ADDs, 2^{K-1} number of *max* operations, and 2^{K-1} look-up tables per a systematic bit [55]. The evaluation of $B_{k-1}(s')$ in (4.26) requires the computational complexity same as that in $A_k(s)$.

The bit-wise LLR estimation in (4.24) needs additional $2^{K+2}+1$ ADDs, $2(2^{K-1}-1)$ numbers of *max* operations, and $2(2^{K-1}-1)$ look-up tables. Note that except the codeword correlation between $x'_{z,k}$ and $x_{z,k}(s', s)$ in $\Gamma_k(s', s)$ each of Log-MAP based turbo decoding computation complexity linearly growth with the number of turbo code iterations and the number of component decoders. Generally, with $mN.N_t$ number of Log-MAP-based STBC soft detection output bits, we have $\frac{mN.N_t}{n}$ systematic bits for turbo decoder input. Therefore, for two-component decoders with a maximum iteration of I, the code rate $R = \frac{1}{n}$, and $\frac{mN.N_t}{n}$ systematic bits the LLR computational requires $C_{Log-MAP}^{TC}$ real MULs, $A_{Log-MAP}^{TC}$ real ADDs, $Max_{Log-MAP}^{TC}$ *max* operations, and $Lt_{Log-MAP}^{TC}$ look-up tables.

$$C_{Log-MAP}^{TC} = \frac{mN.N_t}{n} \left(n.2^K + I.2^{K+1} \right) \tag{4.38}$$

$$A_{Log-MAP}^{TC} = \frac{mN.N_t}{n} \left(2^K (n-1+10I) + 2I \right) \tag{4.39}$$

$$Max_{Log-MAP}^{TC} = \frac{mN.N_t}{n} \left(I.2^{K+1} \right) \tag{4.40}$$

$$Lt_{Log-MAP}^{TC} = \frac{mN.N_t}{n} \left(I.2^{K+1} \right) \tag{4.41}$$

The sum-up receiver complexities of the turbo code and uncoded MIMO-OFDM system with L oversampling, N_t transmitter antennas, N_r receiver antennas, m bits per M-ary QAM symbol, and K constraint length summarizes in Table 4.2. As shown in Table 4.2 compared to the ML algorithm the use of the Log-MAP

algorithm for STBC bit-wise detection and turbo decoding results in additional complexity constraints in all operational aspects of the MIMO-OFDM system.

TABLE 4.2: Uncoded and Turbo code MIMO-OFDM system receiver computational complexity analysis.

Operations	Turbo coded MIMO-OFDM	Uncoded MIMO-OFDM
Real multiplication/ division	$N_r \left(LN \left(\log_2^{LN} - 3 \right) + 4 \right) +$ $N.N_t \left(6m.2^m + 6N_t N_r \right) +$ $\frac{mN.N_t}{n} \left(n.2^K + I.2^{K+1} \right)$	$N_r \left(LN \left(\log_2^{LN} - 3 \right) + 4 \right) +$ $N.N_t \left(5.2^m + 6N_t N_r \right)$
Real addition/ subtraction	$N_r \left(3LN \left(\log_2^{LN} - 1 \right) + 4 \right) +$ $N.N_t \left(m \left(1 + 7.2^m \right) + 6N_t N_r - 2 \right) +$ $\frac{mN.N_t}{n} \left(2^K \left(n - 1 + 10I \right) + 2I \right)$	$N_r \left(3LN \left(\log_2^{LN} - 1 \right) + 4 \right) +$ $N.N_t \left(7.2^m + 6N_t N_r - 2 \right)$
Max	$2mN.N_t \left(2^{m-1} - 1 \right) + \frac{ImN.N_t}{n} \left(2^{K+1} \right)$	$N.N_t \left(2^m \right)$
Look-up tables	$2mN.N_t \left(2^{m-1} - 1 \right) + \frac{ImN.N_t}{n} \left(2^{K+1} \right)$	–

The overall transceiver complexities for the conventional clipping, hybrid PTS [33], and SLM [31] have been obtained by summing up the respective transmitter complexities given in Table 4.1 and the uncoded MIMO-OFDM complexity given in Table 4.2 along with the corresponding operations. Similarly, the TC modified clipping based MIMO-OFDM system's overall complexity has been estimated by adding its transmitter complexity given in Table 4.1 and its receiver complexity given in Table 4.2 along with the corresponding operations.

Chapter 5

Result and Discussion

In this section, the performance of the proposed system has been evaluated using PAPR and BER performance metrics. In turbo code, the BER performance gain has direct proportional with the input data length (also to subcarrier length) [40]. Therefore, for BER performance evaluation a sub-carrier length of N=128 which has the least performance as compared to N=256 and N=512. Therefore, the sub-carrier length of N=128 has been considered for the BER performance evaluation. The effects of the number of quantization levels, step size values, and the number of clipped peak envelopes on the modified clipping MIMO-OFDM system performances have been evaluated. Also, the BER performance of the modified clipping MIMO-OFDM system with different turbo code iterations has been shown.

Further apart from this, the overall complexity of the proposed system with respect to various existing works has been evaluated. Finally, to give some highlights and understandings the proposed system performances have been compared with some of the common and recent works. Table 5.1 presents the list of the common parameters utilized in the performance metrics evaluation of the TC modified clipping MIMO-OFDM system.

TABLE 5.1: Parameters use in simulation

No	Parameters	Symbols	Values /Types
1	Number of sub-carriers	N	128, 256, 512
2	Generator polynomial	G	$g_1 = 17_{oct}$,$g_2 = 15_{oct}$
3	Constraint length	K	4
4	Trellis termination bits	-	12
5	Turbo code rate	R	1/3
6	Turbo interleaver/deinterleaver	-	Random
7	Modulation scheme	-	8-QAM
8	Transmitter antennas	N_t	1, 2
9	Receiver antennas	N_r	1, 2, 3, 4, 8
10	Length of cyclic prefix	$N_{cp} = \frac{N}{4}$	32, 64, 128
11	Oversampling factor	L	4
12	STBC detection algorithm	-	Log-MAP
13	Turbo decoding algorithm	-	Log-MAP
14	Number of iterations	-	1, 2, 3, 4, 5

5.1 Performance of Uncoded and TC MIMO-OFDM System

The simulation result in Figure 5.1 illustrates the PAPR for uncoded and turbo code STBC MIMO-OFDM systems with different numbers of sub-carriers. The PAPR performance of MIMO-OFDM system depends on sub-carrier length. As the sub-carrier N increases the PAPR becomes large. For example at a reference CCDF value of 5×10^{-4} the PAPR increase by $0.4dB$ and $0.7dB$ for $N = 256$ and $N = 512$ respectively as compared to the PAPR of $N = 128$. The figure also shows the CCDF curve for uncoded and coded MIMO-OFDM systems exactly overlap to each other among respective sub-carrier especially for $N = 128$. While for large sub-carrier ($N = 512$) the turbo interleaver plays a role to make the component encoder outputs uncorrelated. This low correlation between transmitted symbols, thus result in a small PAPR reduction gain as compared to the uncoded system.
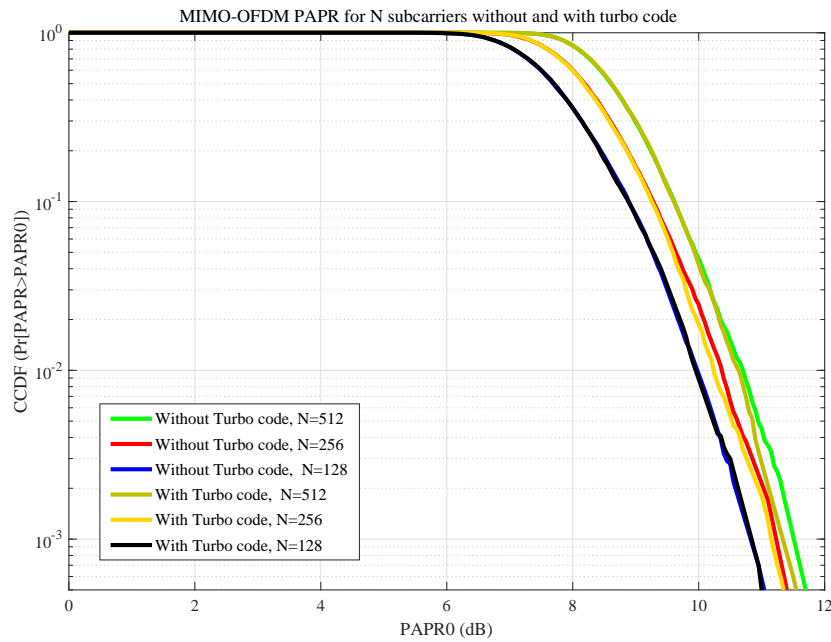
FIGURE 5.1: CCDF of STBC MIMO-OFDM with and without turbo code for different sub-carrier length ($N = 128, 256, 512$)

Figure 5.2 shows the BER performances of uncoded $N_t \times N_r$ OFDM system for $N = 128$. As expected, the BER performance of the OFDM system has been enhanced using STBC diversity. Therefore, the combination of MIMO with OFDM result in reliable wireless communication.
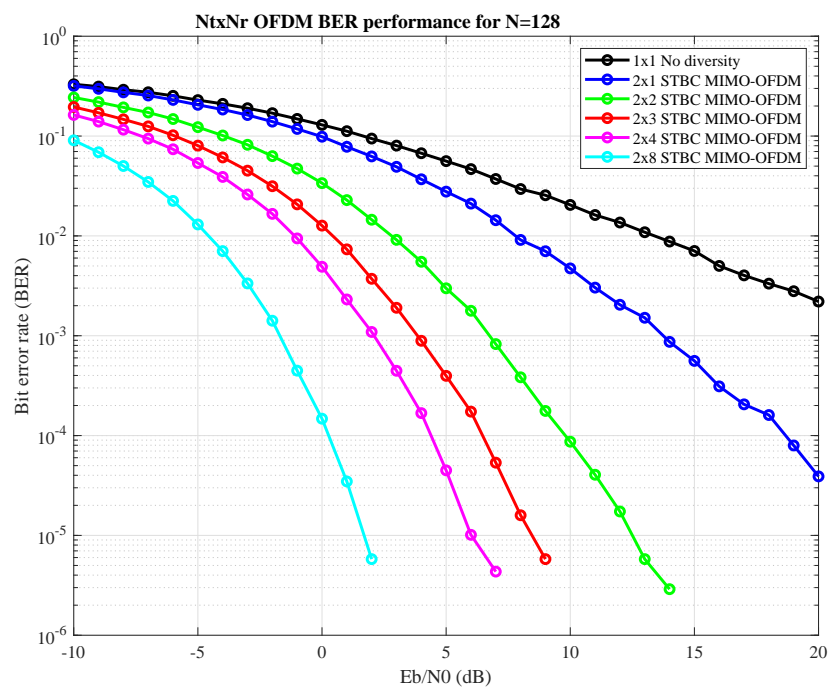

FIGURE 5.2: BER performance of $N_t \times N_r$ OFDM system.

Figure 5.3 presents the BER performances of 1st and 2nd iteration TC $N_t \times N_r$ OFDM system for $N = 128$. The simulation result proves that the integration of turbo code to $N_t \times N_r$ OFDM system results in additional BER gain over its respective uncoded $N_t \times N_r$ OFDM system depicted in Figure 5.2. For example, at 1×10^{-4} BER reference value the E_b/N_0 gains of TC MIMO-OFDM system with respect to the uncoded MIMO-OFDM system present in Table 5.2.
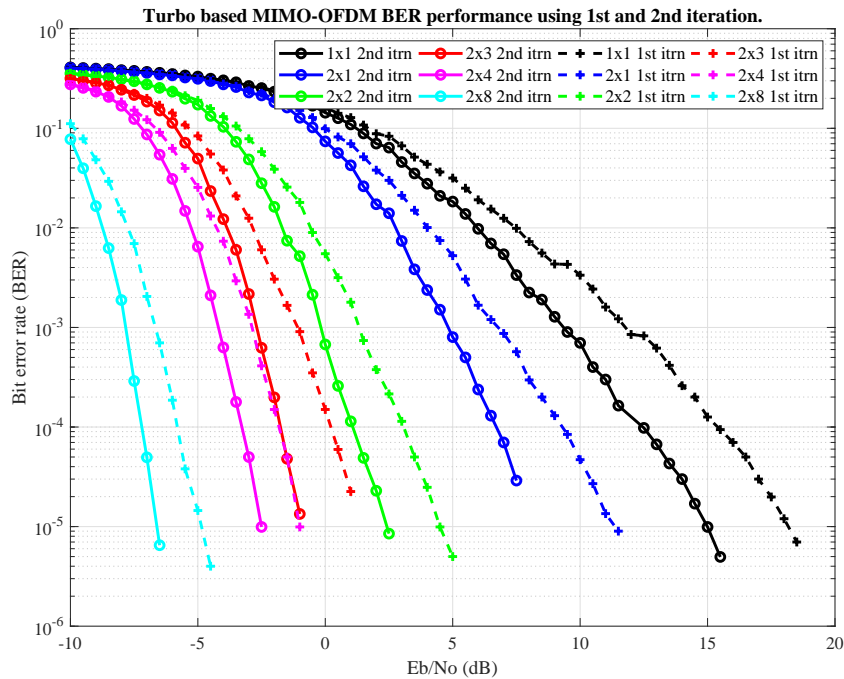
FIGURE 5.3: BER performance of $N_t \times N_r$ OFDM system with 1st and 2nd iteration turbo coding for $N = 128$.

TABLE 5.2: Uncoded, 1st iteration TC, and 2nd iteration TC $N_t \times N_r$ OFDM system E_b/N_0 at a reference BER of 1×10^{-4}.

$N_t \times N_r$	Uncoded E_b/N_0	1st iteration E_b/N_0	2nd iteration E_b/N_0	1st iteration gain in dB over uncoded	2nd iteration gain in dB over uncoded	2nd iteration gain in dB over 1st iteration
1×1	-	15.38	12.46	-	-	2.92
2×1	18.67	9.303	6.711	9.367	11.959	2.592
2×2	9.8	3.08	1.076	6.72	8.724	2.004
2×3	6.468	0.22	-1.717	6.248	8.185	1.937
2×4	4.392	-1.815	-3.274	6.207	7.666	1.459
2×8	0.269	-5.824	-7.2	6.093	7.469	1.376

5.2 Performance of MIMO-OFDM System Using Conventional Clipping

The PAPR performance in the MIMO-OFDM system using conventional clipping has shown in Figure 5.4. The simulation result presents for the clipping ratio of $\gamma = (9,\ 8,\ 7)$ dB. The results in the figure reveal the PAPR of the system has a direct relationship to that of γ value.
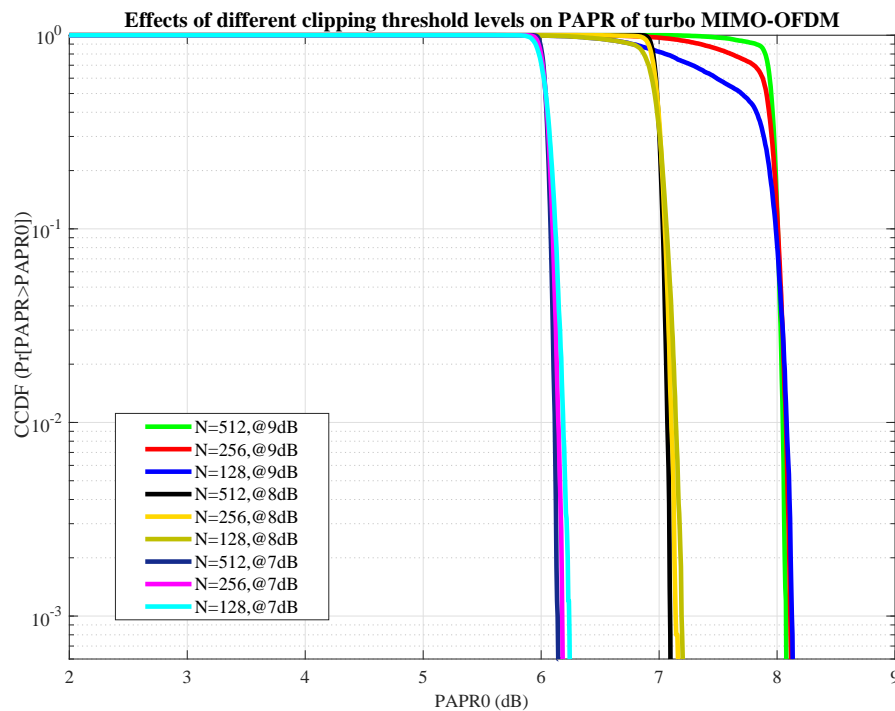
FIGURE 5.4: CCDF of turbo based MIMO-OFDM using conventional clipping with clipping ratios $\gamma = (9,\ 8,\ 7)\,dB$ for sub-carrier length $N = (128,\ 256,\ 512)$.

From the simulation result the original $11dB$ PAPR value ($CCDF = 5 \times 10^{-4}$) for sub-carrier $N = 128$ has been improved by $2.8dB$, $3.8dB$ and $4.8dB$ using a sequential clipping ratio γ values of $9dB$, $8dB$ and $7dB$. When the sub-carrier increases the improvements of PAPR for a given clipping ratio γ increases as compared to the improvements for sub-carrier $N = 128$ along with the corresponding γ value.

Figure 5.5 shows the BER of uncoded $N_t \times N_r$ OFDM using a conventional clipping having a γ value of $7dB$. As expected, clipping more probably deteriorates the BER of high order diversity the MIMO-OFDM system. This happens due to the direct proportionality of clipping distortion with the diversity order of MIMO-OFDM system. Also as the γ value decreases more to get better reduction gain in PAPR the BER performance deteriorates in severe especially for higher-order diversity.

FIGURE 5.5: BER performance of uncoded $N_t \times N_r$ OFDM system using conventional clipping with $\gamma = 7$dB.

5.3 Performance of MIMO-OFDM Using Different Quantization Levels

The number of quantization levels effects on PAPR performance of modified clipping TC MIMO-OFDM system has shown in Figure 5.6 and also summarized in Table 5.3. The number of quantization levels has inversely related to the PAPR performance. When the number of quantization levels increases the number of selected peak envelopes for clipping has less probability to cutoff deeply. This

deteriorates PAPR reduction gain. While as the number of quantization levels decrease the selected peak envelopes for clipping have a high probability to cutoff deeply and this result in a better PAPR reduction gain.
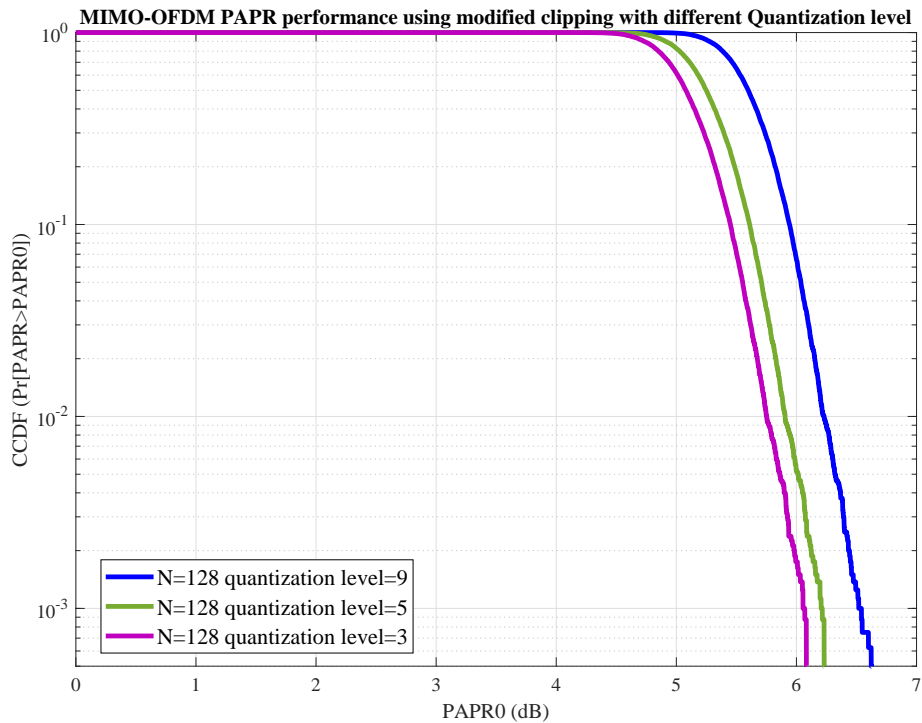
FIGURE 5.6: TC MIMO-OFDM CCDF using modified clipping having 9, 5, 3 quantization levels and 0.05 step size with 5% of high peak envelope clipped for sub-carrier N=128.

TABLE 5.3: Effects of the number of quantization levels in modified clipped MIMO-OFDM PAPR performance.

Modified clipping parameters			PAPR value in dB @ CCDF of 5×10^{-4} for sub-carrier N=128	Gains of modified clipping over the original MIMO-OFDM system
Number of quantization levels	Step size value	Clipped peak envelopes		
3	0.05	5%	6.1	4.9
5	0.05	5%	6.2	4.8
9	0.05	5%	6.6	4.4

Figure 5.7 presents the impacts of quantization levels on the BER performance of modified clipping $N_t \times N_r$ OFDM system. The number of quantization levels directly proportional to the BER performance. Also, the result reveals the use of quantization level in modified clipped has more important for high order diversity MIMO-OFDM system while the BER in a non-diversity OFDM system is almost constant irrespective of quantization level numbers.

MIMO-OFDM BER performance using modified clipping with 3 and 9 quantization levels
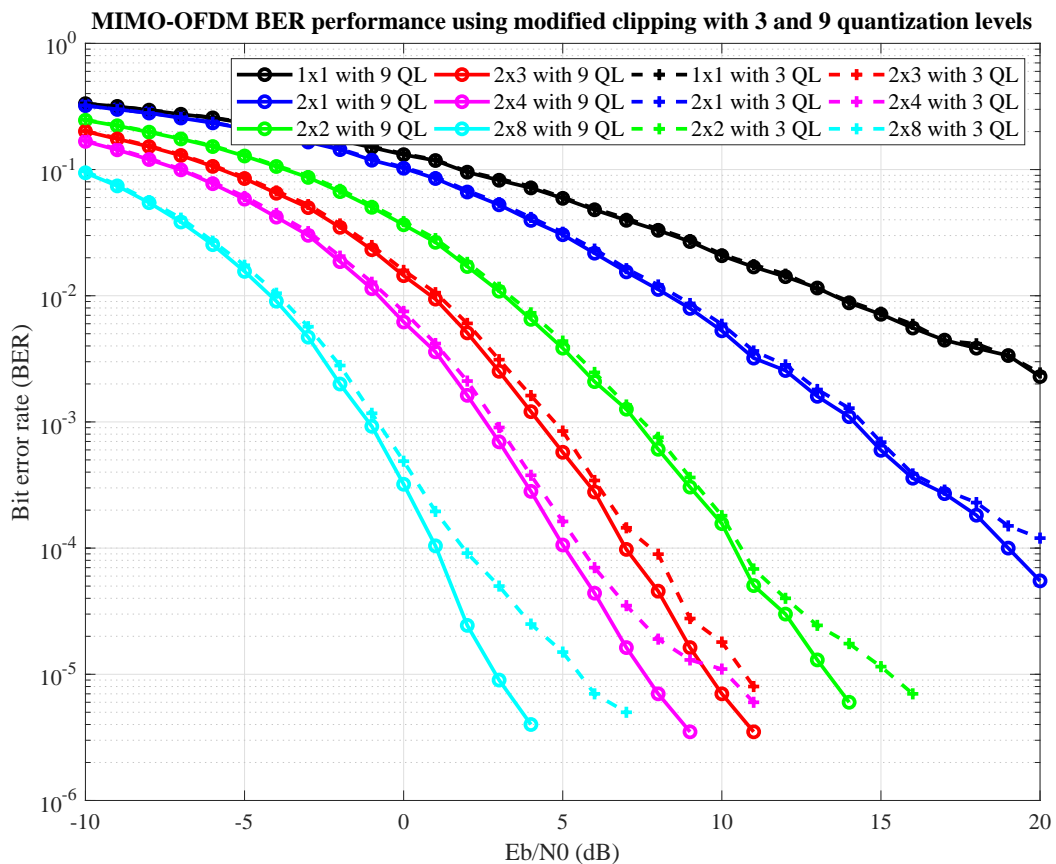
FIGURE 5.7: BER performance of uncoded $N_t \times N_r$ OFDM system using modified clipping having 3, 9 quantization levels, 5% clipped peak envelopes, and 0.05 step size value.

As presented in Figure 5.7 modified clipping having 5 quantization levels, 0.05 step size value, and 5% high peak clipped envelopes has a PAPR performance which is moreover approaching the conventional clipping with a clipping ratio of 7dB, see Figure 5.4. Figure 5.8 shows their comparative BER performance. As shown from the figure modified clipping results in a slightly better BER gain. This gain comes due to the usage of quantization levels. Since quantization levels allow a better

probability to de-mapping some of clipped $N_t \times N_r$ OFDM symbols (especially for high diversity order) to the corresponding true constellation symbols. As the result, modified clipping having comparable PAPR performance with convectional clipping has slightly preferable BER performance, especially for high diversity order.
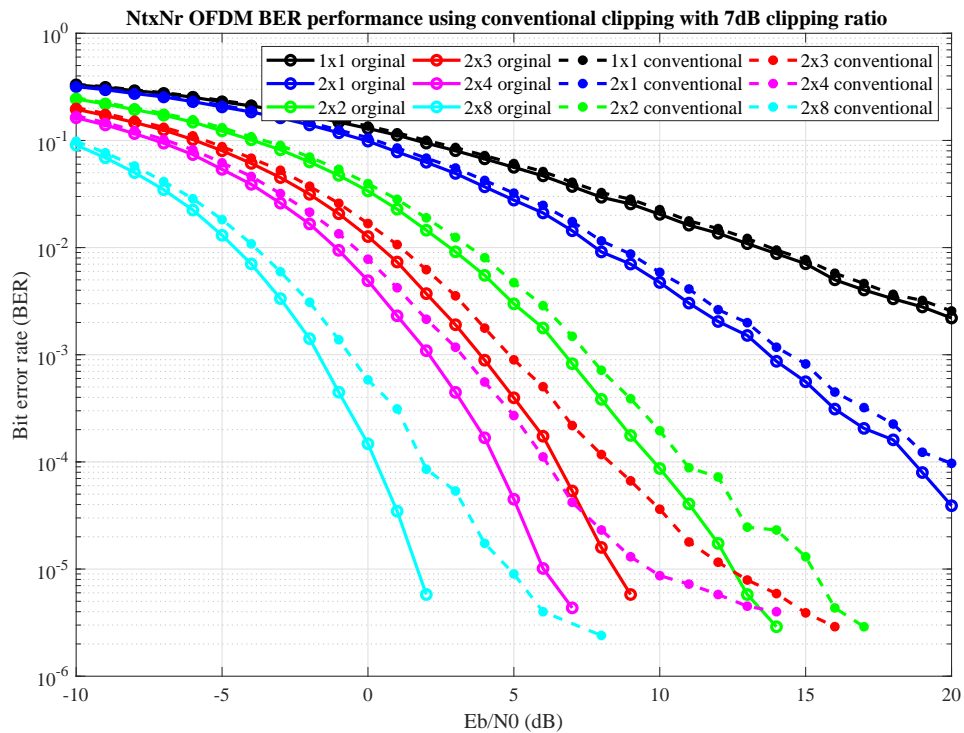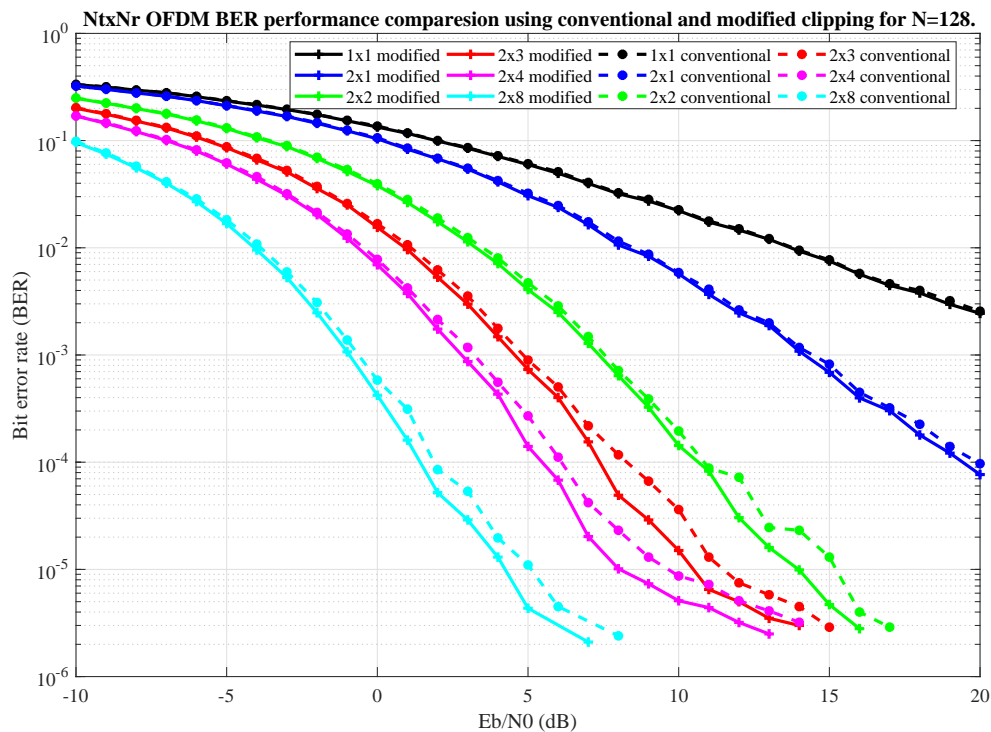

FIGURE 5.8: BER performance of uncoded $N_t \times N_r$ OFDM system using conventional clipping with $\gamma = 7$dB and modified clipping with 5% clipped peak envelopes, 5 quantization levels, and 0.05 step size.

5.4 Performance of MIMO-OFDM Using Different Step Size Value

The modified clipping MIMO-OFDM system performances are affected by step size value in a similar way to that of the number of quantization levels. This means a high step size value enhances BER with deteriorated PAPR reduction gain. While if the step size value is too small a better PAPR reduction gain has been achieved at the cost of BER performance. Figure 5.9 and Table 5.4 presents the effects of step size values on the modified clipping MIMO-OFDM system PAPR performance.

The figure and table illustrate the inverse relationship of PAPR reduction gain with step size value.
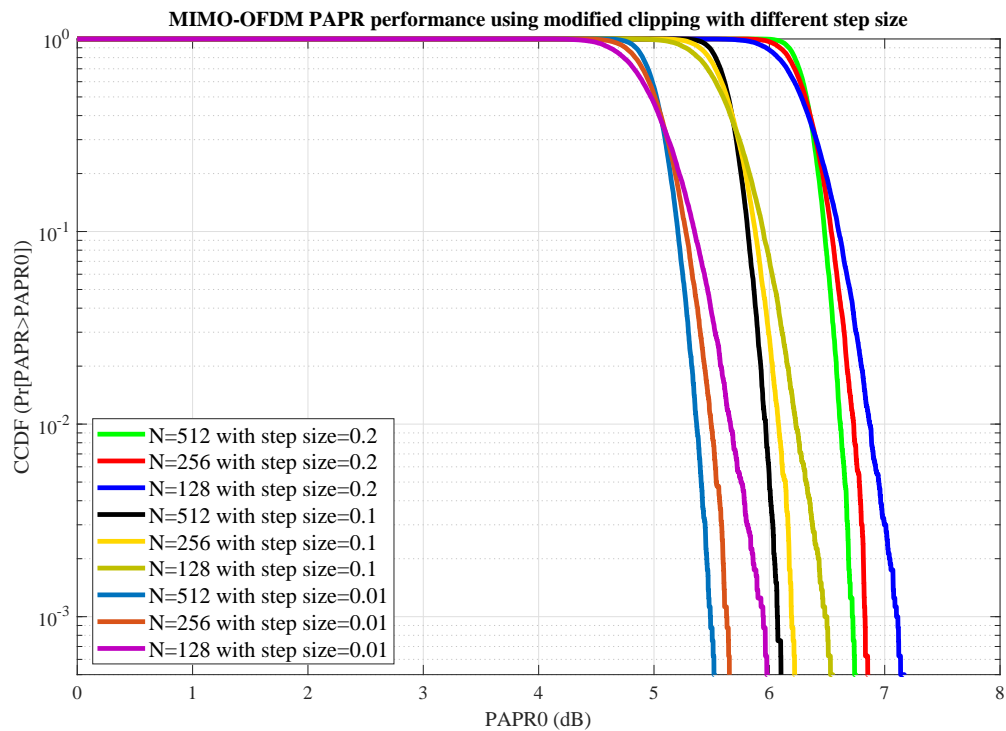
FIGURE 5.9: TC MIMO-OFDM CCDF using modified clipping having 0.2, 0.1, 0.01 step size values, 5 quantization levels, and 5% of high peak envelope clipped in each sub-carrier.

TABLE 5.4: Effects of step size values in modified clipping MIMO-OFDM PAPR performance.

Modified clipping parameters			PAPR values in dB @ CCDF of 5×10^{-4} for sub-carrier N= {128, 256, 512}			Gain of modified clipping over orginal MIMO-OFDM in dB		
Number of quantiz- ation levels	Step size value	Clipped peak envelopes	128	256	512	128	256	512
5	0.01	5%	6	5.6	5.5	5	5.8	6.2
5	0.1	5%	6.5	6.2	6.1	4.5	5.2	5.6
5	0.2	5%	7.2	6.9	6.8	3.8	4.5	4.9

Figure 5.10 presents the BER performance of the uncoded modified clipping $N_t \times N_r$ OFDM system with 0.01 and 0.2 step size values. As expected the BER with

a high step size value i.e. 0.2 results in a better BER performance as compared to the small step size value i.e. 0.01.

FIGURE 5.10: BER performance of uncoded $N_t \times N_r$ OFDM system using modified clipping having 5% high peak clipping with 0.01, 0.2 step sizes, and 5 quantization levels.

5.5 Performance of MIMO-OFDM Using Different Clipped Envelopes

As compared to the step size values and the number of quantization levels the number of clipped peak envelopes has an opposite role on the performances of modified clipping MIMO-OFDM system i.e large number of clipped peak envelopes results in better PAPR reduction gain with high BER loss. Figure 5.11 illustrates the effects of the number of clipped peak envelopes on TC MIMO-OFDM PAPR performance. From the CCDF figure, using 10% clipped high peak envelope the PAPR of the original MIMO-OFDM system has been improved by 53.64%, 57.02%, and 58.97% for sequential order of 128, 256, and 512 sub-carriers. As the numbers of clipped peak envelopes increases to 20% and 25% the PAPR of the original

MIMO-OFDM system has been reduced by 65.45%, 66.67%, and 69.23% and by 69.09%, 71.05%, and 72.65% for each respective sub-carriers of 128, 256, and 512.
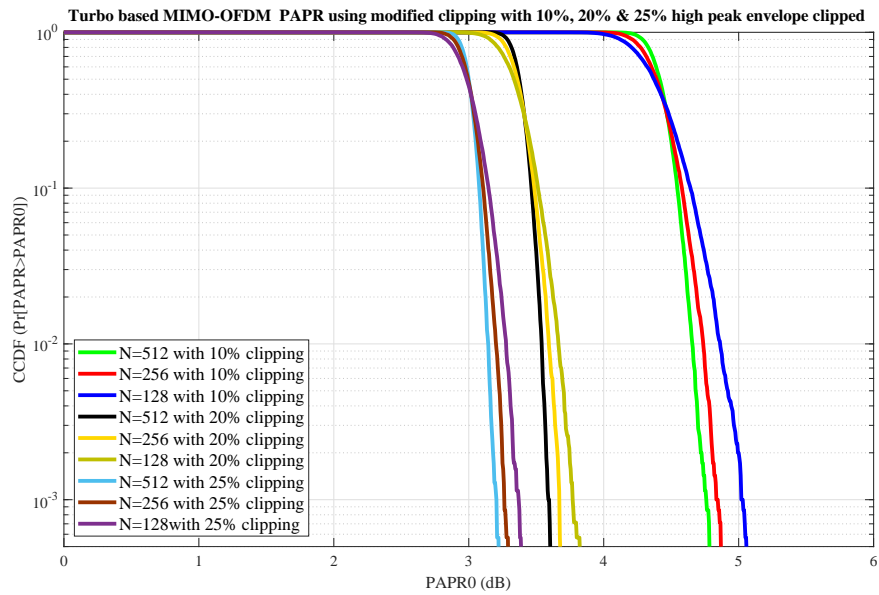
FIGURE 5.11: CCDF of TC MIMO-OFDM using modified clipping having 5 quantization levels and 0.05 step size value with 10%, 20%, and 25% high peak clipping in each sub-carriers.
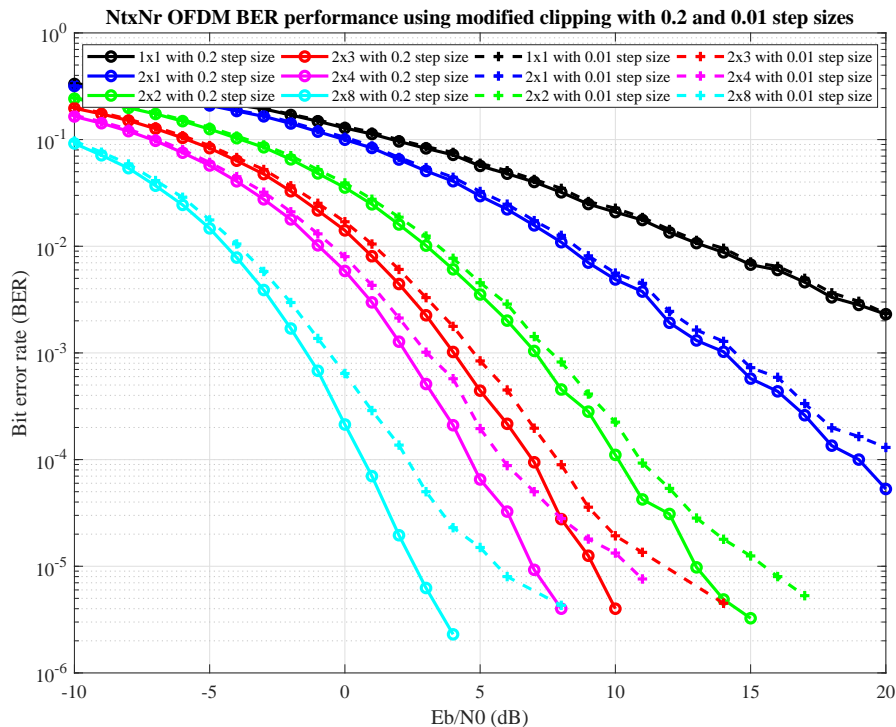

FIGURE 5.12: BER performance of uncoded $N_t \times N_r$ OFDM system using modified clipping having 10% and 25% high peak clipping with 5 quantization levels and 0.05 step size value.

Figure 5.12 shows the effects of the numbers of clipped high peak envelopes on the BER performance of $N_t \times N_r$ OFDM system. From the figure, $N_t \times N_r$ OFDM system BER performance becomes worse (more prominent for high diversity order) when a large number of signal peaks have been clipped especially at 25% of the peak envelopes have clipped. At this stage, the loss of BER is more as compare to the PAPR reduction gain. As the result, the use of modified clipping with 25% clipped high peak envelopes become insignificant.

5.6 Modified Clipping MIMO-OFDM System Performance with Turbo Code

Figure 5.13 presents the BER performance of 1st iteration turbo code $N_t \times N_r$ OFDM system with 5% and 25% of clipped peak envelopes. For both clipped peak envelopes the simulation has depicted using 5 quantization levels and 0.05 step size value.

FIGURE 5.13: BER performance of 1st iteration turbo code $N_t \times N_r$ OFDM system using modified clipping having 5% and 25% of high peak clipping with 5 quantization levels and 0.05 step size value.

The concatenation of turbo code to the MIMO-OFDM system allows a significant advantage for modified clipping $N_t \times N_r$ OFDM system having severe BER loss (e.g 25% of peak clipping shown in Figure 5.12). The improvement happens due to the effective recovery of transmitted data from clipping and channel distorted received data through the Log-MAP turbo decoding process. This results in better BER gain over the uncoded system with and without modified clipping. As compared to the TC $N_t \times N_r$ OFDM syste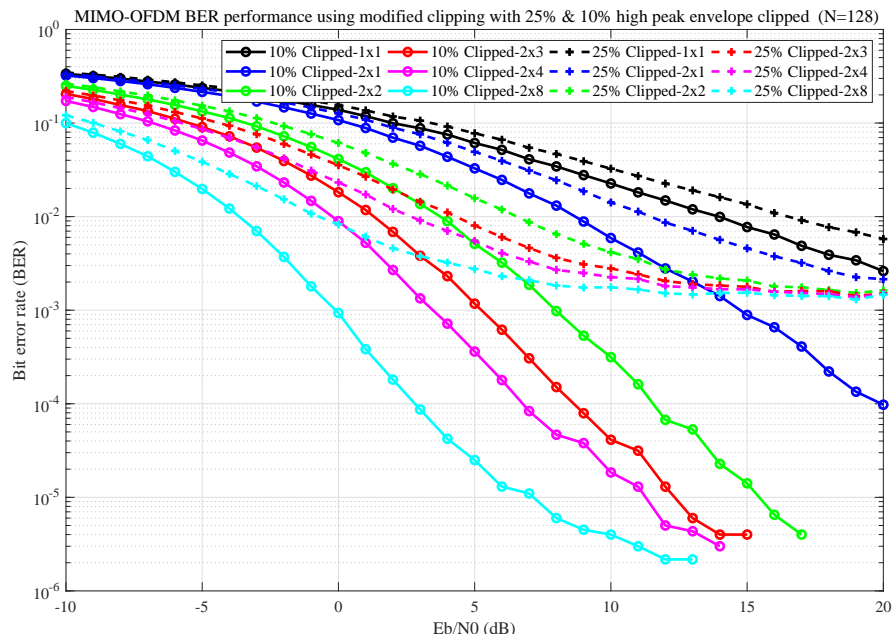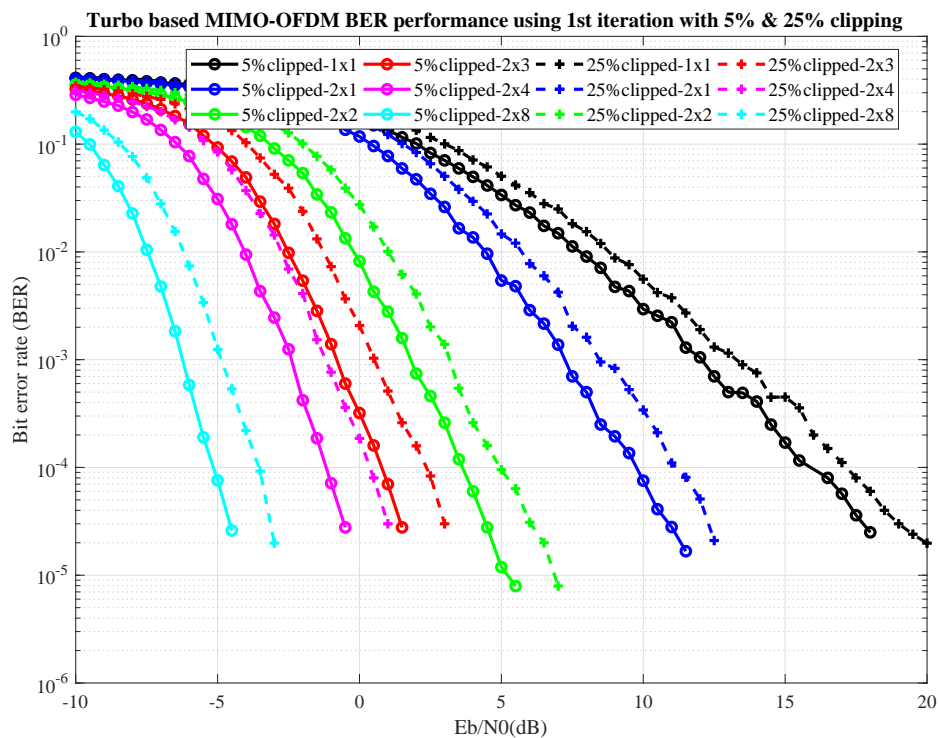m the modified clipping TC $N_t \times N_r$ OFDM system results in some BER performance penalty, which is proportional to amounts of clipped peak envelopes. Table 5.5 shows the performances of the proposed system using the first TC iteration with respect to the first iteration TC MIMO-OFDM and uncoded MIMO-OFDM system at 1×10^{-4} BER reference value.

TABLE 5.5: 1st iteration TC modified clipping $N_t \times N_r$ OFDM system E_b/N_0 with respect to uncoded and 1st iteration TC $N_t \times N_r$ OFDM system at a BER reference value of 1×10^{-4}.

$N_t \times N_r$	TC modified clipping E_b/N_0 @1×10^{-4} BER		Gain in dB over $N_t \times N_r$ OFDM system		Loss in dB over 1st TC $N_t \times N_r$ OFDM system	
	25%	5%	25%	5%	25%	5%
1×1	17.16	15.83	-	-	1.78	0.45
2×1	11.15	9.812	7.52	8.858	1.847	0.509
2×2	4.952	3.67	4.848	6.13	1.872	0.59
2×3	2.354	0.841	4.114	5.627	2.135	0.622
2×4	0.353	-1.176	4.039	5.568	2.168	0.639
2×8	-3.556	-5.167	3.825	5.436	2.268	0.657

The E_b/N_0 gain at a given BER for TC modified clipping $N_t \times N_r$ OFDM system can be enhanced indeed more than the one depicted in Figure 5.13 by utilizing turbo log-MAP decoding with the second iteration. Figure 5.14 proves this. For example, at BER reference value of 1×10^{-4} using 5% clipped envelopes the E_b/N_0 gains of $3.18dB$, $2.752dB$, $2.275dB$, $2.175dB$, $1.718dB$, and $1.689dB$ have gotten over its corresponding first iteration in the respective transmitter and receiver antenna combination of 1×1, 2×1, 2×2, 2×3, 2×4, and 2×8 OFDM system. For the 25% clipped envelopes the E_b/N_0 gains of $2.92dB$, $2.294dB$, $2.131dB$,

2.065dB, 1.693dB and 1.624dB have gotten over its corresponding first iteration in the respective transmitter and receiver antenna combination of 1×1, 2×1, 2×2, 2×3, 2×4, and 2×8.
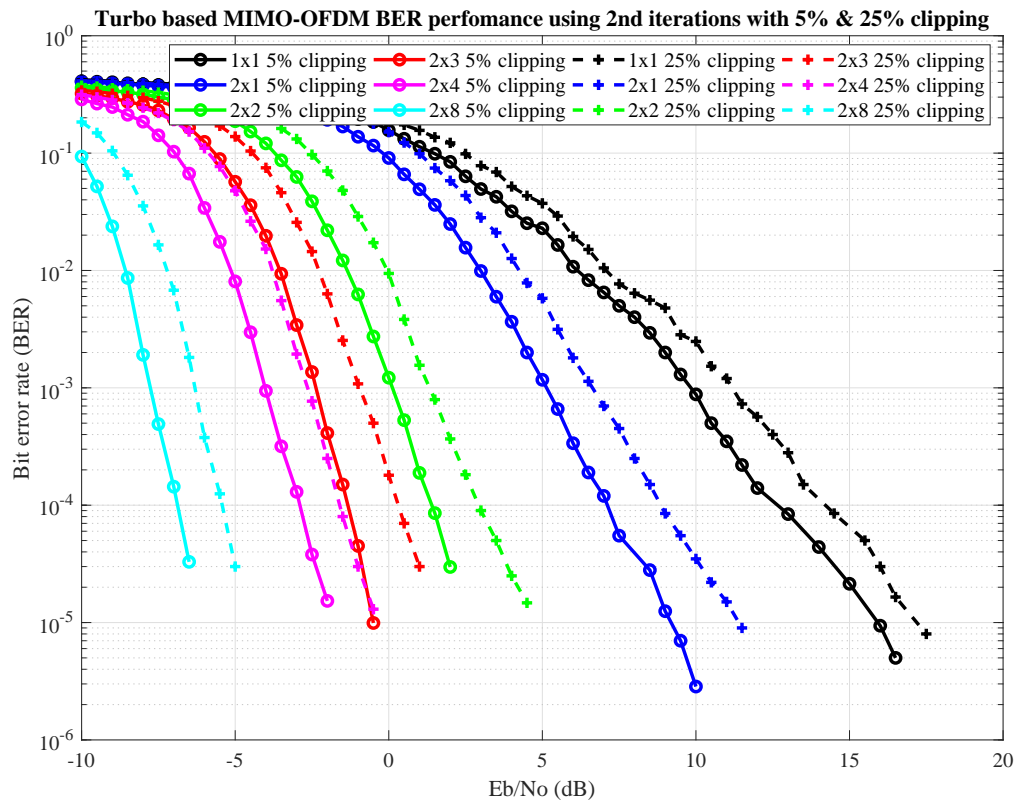
FIGURE 5.14: BER performance of 2nd iteration turbo code $N_t \times N_r$ OFDM system using modified clipping having 5% and 25% clipped envelopes with 5 quantization levels and 0.05 step size value.

Figure 5.15 shows the effects of turbo code iterations on the BER performances of the modified clipping MIMO-OFDM system. The simulation has done for turbo code based 2×8 modified clipping MIMO-OFDM system using 5%, 25% clipped envelopes, 5 quantization levels, and 0.05 step size value. As the figure illustrates with the continuous increments of TC iteration the BER performances of each respective TC modified clipping MIMO-OFDM system have been improved on average. However, the BER performance gains for each additional iteration carried out have declined and after some iteration order, the performance gain becomes converged and insignificance (just after five iterations in Figure 5.15). Therefore,

to average out the complexity of turbo decoders with the convergence BER performance gain, in this thesis work, a maximum of five iterations are carried out.
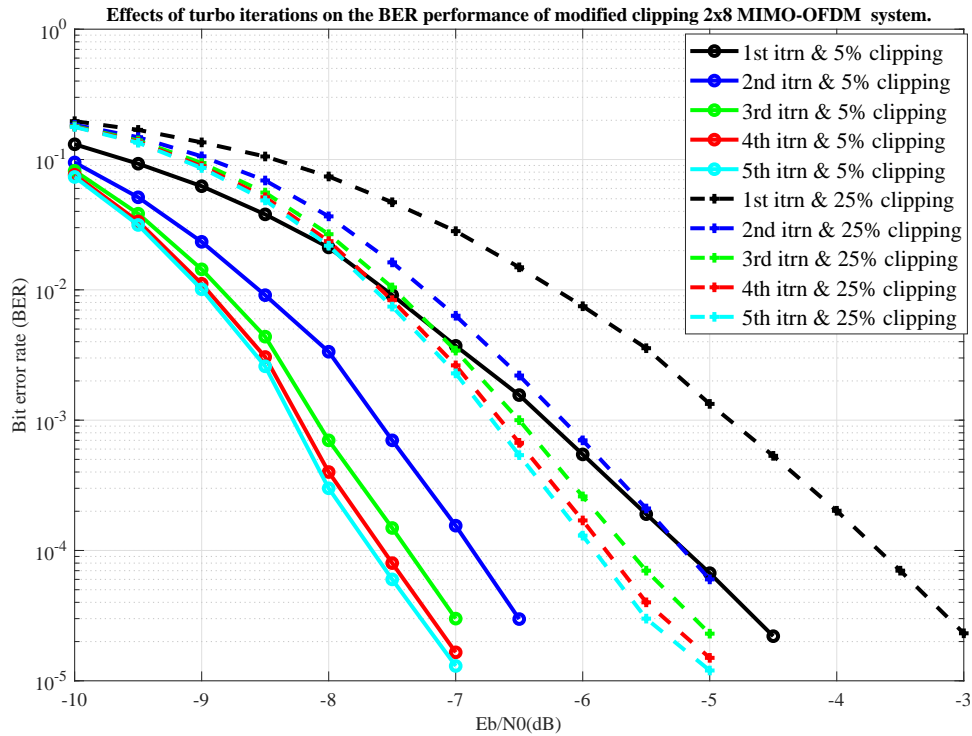
FIGURE 5.15: Effects of TC iterations on the BER performance of turbo code MIMO-OFDM system using modified clipping having 5% and 25% clipped envelopes with 5 quantization levels and 0.05 step size value.

5.7 Proposed System Complexity

Figure 5.16 shows the complexity comparison of the TC modified clipping based proposed system and the various existing PAPR reduction works like hybrid PTS [33], SLM [31], and conventional clipping in terms of the required number of real multiplications. As presented in subsection 4.3 the overall proposed system complexity uniquely depends on the order of the clipped envelopes, quantization levels, constraint lengths, and TC iteration. While both the proposed work of this thesis and the existing works of hybrid PTS [33], SLM [31], and conventional clipping complexities commonly depend on the length of sub-carrier, the order of M-ary modulation, and also on both the transmitter and receiver antenna orders.

In Figure 5.16 the required real multiplications in the proposed system model and all the existing works have been evaluated using $N_t = 2, N_r = 8$, and 8-QAM modulation for the various sub-carrier length. The sub-block length of $V = 8$ has been considered for hybrid PTS in [33] while for SLM in [31] the four sub-block lengths with contiguous extended sub-blocks of $C = 4$, and a unity basic data unit sub-block have been used as suggested by the respective cited works. For the case of the proposed system complexity simulation, the worst scenario has been considered (i.e. with 5th TC iteration and 25% clipped envelopes) using 5 quantization levels.
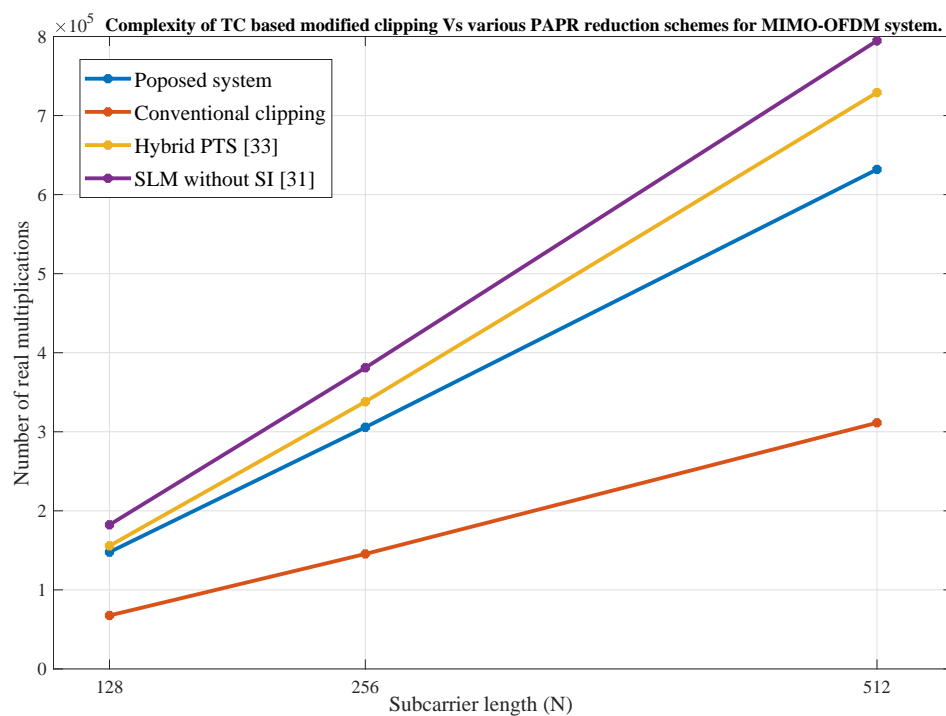
FIGURE 5.16: Comparison of the TC modified clipping based proposed MIMO-OFDM system overall complexity with the uncoded various PAPR reduction scheme based MIMO-OFDM system complexities.

As the above figure illustrates, the proposed system needs fewer real multiplication complexity constraints as compared to the presented works of hybrid PTS in [33] and SLM in [31]. On the other hand, the proposed system of this thesis work requires more real multiplication complexity constraints as compared to the conventional clipping MIMO-OFDM system. This complexity constraint of the TC modified clipping proposed system mainly comes due to the use of Log-MAP based bit-wise STBC detection and Log-MAP based turbo decoder.

5.8 Proposed System Performance with the Existing Works

The comparison of the proposed system performance with existing PAPR reduction techniques has been difficult since the proposed system parameters differ from the parameters used in those methods. However, for the evaluation scenario, the proposed systems compare to the most common and the recent existing MIMO-OFDM PAPR reduction methods as shown in Table 5.6. The proposed system having 5 quantization levels, 0.05 step size value, and 25% clipped peak envelopes shown in Figure 5.11 has been used for PAPR comparison. For BER comparison TC modified clipping MIMO-OFDM system with iteration $1 < I \leq 5$ has taken.

Like most PAPR reduction methods in the designed modified clipping, the trade-off exists between PAPR reduction gain and BER performance. This trade-off is significantly compromised by integrating the designed modified clipping with a powerful channel coding. As a result, the clipping distortion has been minimized and a better BER performance with outstanding PAPR reduction gain has achieved. Therefore, as compared to the reported work in [22, 29, 31, 33] the proposed system has remarkable PAPR reduction gain with exaggerated better BER performance.

In [18] the PAPR performance mainly depends on μ value and the best result of $3dB$ at $\mu = 255$ was obtained. However, this result at $\mu = 255$ has not been recommended by the author as it introduces high BER loss. Therefore, $\mu = 100$ has been chosen to compromise the PAPR and BER performances. Using this value of μ $3.5dB$ PAPR has been achieved and this has more than $0.1dB$ loss as compared to the PAPR reduction gain of the proposed system. In [15] the PAPR reduction gain subjects to convolutional code, CARI as well as to iteratively modified μ companding and filtering. Using filtered signal with 3 iterations the author has gotten the best PAPR reduction gain of $7dB$ for sub-carrier 128. This result has a loss of $0.6dB$ as compared to the result of this thesis work. On the other hand,

the proposed system has an outstanding BER performance over the reported work given in [15] while the special case of [18] has a comparable BER performance.

TABLE 5.6: Proposed system PAPR reduction gain performance comparison with existing PAPR reduction woks.

PAPR reduction method	Parameters			CCDF value	PAPR in dB @ CCDF value
	Modulation	N	$N_t \times N_r$		
Proposed turbo code modified clipping	8QAM	128,256, 512	2×8	5×10^{-4}	$3.2 \leq PAPR_0 \leq 3.4$
SLM without SI [31]	QPSK, 16QAM	512	$N_t = 2$	10^{-3}	$8 < PAPR_0 < 9$
Time domain cyclic SLM with CC [29]	QPSK	128	$N_t = 2, 4$	10^{-3}	$9 < PAPR_0 < 10$ Depends on N_t
Companding with polar code [18]	QPSK	64,128, 256, 512 , 1024	2×2	10^{-4}	$3 \leq PAPR_0 < 7$ Depends on μ value
CC, CARI iterative companding & filtering [15]	QPSK	128	2×2	10^{-4}	$4 < PAPR_0 < 9$ Depends on μ
Adaptive clipping [22]	QPSK, 4QAM	128	2×1	6×10^{-2}	$PAPR_0 \approx 5$
Hybrid PTS [33]	QPSK	128	$N_t = 2$	10^{-4}	$6 < PAPR_0 < 11$

Generally, as compared to the above PAPR reduction work presented in Table 5.6 the proposed system work attain a significant BER performance gain with remarkable PAPR reduction gain and reasonable moderate computational complexity.

Chapter 6

Conclusion and Recommendation

6.1   Conclusion

MIMO-OFDM system has been adopted in many wireless standards and applications. The MIMO-OFDM system allows to using the sum-up advantages of the MIMO and OFDM systems. Despite its benefits, the MIMO-OFDM system has the disadvantage of having a high PAPR. High PAPR degrades the performance of non-linear devices such as the HPA, resulting in BER loss and spectral splatter. To address this issue numerous techniques have been explored by different researchers. Signal distortion is just one of those techniques that gets attention due to its considerable PAPR reduction ability, low complexity, and spectral efficiency (since no side information is required). Clipping is one of the most simple SD techniques, and it achieves remarkable PAPR reduction gains at low threshold levels. Clipping, on the other hand, causes severe BER performance loss at low threshold levels (better PAPR reduction gain).

To address the limitation of conventional clipping the integration of the designed modified clipping with turbo code was explored in this thesis work. The simulation results have been done under different parameters of the designed modified clipping technique. From the proposed demonstration result, we generalized the following:

- The use of conventional clipping with small values of clipping ratio to get remarkable PAPR gain leads the severe BER performance degradation, especially in the high-order diversity MIMO-OFDM systems.

- The use of turbo code in the MIMO-OFDM system allows some PAPR gain for large subcarrier (N=512) over the original PAPR.

- In this thesis, the proposed modified clipping PAPR reduction gain has a direct relationship with the numbers of clipped high peak envelopes and an inverse relationship with the number of quantization levels and step size values. While the BER performance has been related with these modified clipping parameters in the reverse manner of PAPR reduction gain.

- For high diversity order STBC MIMO-OFDM systems, the designed modified clipping has better BER performance than conventional clipping at a comparable PAPR reduction gain.

- Modified clipping with 5 quantization levels, 0.05 step size value and 25% of clipped high peak envelopes the PAPR reduction gain of 69.09%, 71.05%, and 72.65% have achieved for a sequential sub-carrier 128, 256, and 512. However, under these parameters value modified clipping become useless since the loss in BER is greater as compared to PAPR gain.

- The integration of modified clipping having extreme parameter values (for example with 25% of clipped high peak envelopes) to the turbo code results in an outstanding BER performance with remarkable PAPR reduction gain.

- The proposed system work attain a significant compromise of the BER performance and the PAPR reduction gain trade-off over the existing PAPR reduction works with a reasonable moderate computational complexity.

6.2   Recommendation

Compared to the existing conventional clipping alone, the proposed modified clipping method with turbo coding has remarkable PAPR and BER performances.

In this thesis work, turbo code has been used for the purpose of BER performance enhancement. However, like other channel coding techniques turbo code can also use for PAPR reduction with additional complexity constraints. Therefore, MIMO-OFDM PAPR reduction using turbo code would be recommended in future work. Further part to this, in the proposed thesis work, a random interleaver with a relatively low memory size (i.e. 4) has been used. In order to improve the PAPR further, the estimation of turbo code generator polynomials having minimum correlation is necessary. Therefore, generator polynomials with a minimum correlation for a given memory size should consider in future work. Also, in this work, a perfect channel state information has been assumed but this is not practical. Therefore, in future work, the channel estimation either alone or in conjunction with the turbo decoder algorithm would be recommended. Additionally, for future TC modified clipping can integrate with other PAPR reduction techniques to get additional PAPR reduction gain.

Bibliography

[1] Rahman, Muhammad Imadur, Suvra Sekhar Das, and Frank HP Fitzek. "OFDM based WLAN systems." Center for TeleInFrastruktur (CTIF), Aalborg University, Tech. Rep (2005).

[2] L. Litwin, "An introduction to multicarrier modulation," in IEEE Potentials, vol. 19, no. 2, pp. 36-38, April-May 2000, doi: 10.1109/45.839645.

[3] Bulusu, Sri Satish Krishna Chaitanya. Performance analysis and PAPR reduction techniques for filter-bank based multi-carrier systems with non-linear power amplifiers. Diss. Conservatoire national des arts et metiers-CNAM, 2016.

[4] Fettweis, Gerhard, Marco Krondorf, and Steffen Bittner. "GFDM-generalized frequency division multiplexing." VTC Spring 2009-IEEE 69th Vehicular Technology Conference. IEEE, 2009.

[5] Rani, P. Naga, and Ch Santhi Rani. "UFMC: The 5G modulation technique." 2016 IEEE international conference on computational intelligence and computing research (ICCIC). IEEE, 2016.

[6] Zhang, Lei, et al. "Filtered OFDM systems, algorithms, and performance analysis for 5G and beyond." IEEE Transactions on Communications 66.3 (2017): 1205-1218.

[7] Di Stasio, Francesco, Marina Mondin, and Fred Daneshgaran. "Multirate 5G downlink performance comparison for f-OFDM and w-OFDM schemes with different numerologies." 2018 international symposium on networks, computers and communications (ISNCC). IEEE, 2018.

[8] Pasha, Syed Gilani, and Vinayadatt V. Kohir. "OFDM based DVB-T system implementation using MATLAB and HDL coder." 2017 International Conference on Computing Methodologies and Communication (ICCMC). IEEE, 2017.

[9] Al-Dweik, Arafat, et al. "Efficient interleaving technique for OFDM system over impulsive noise channels." 21st Annual IEEE international symposium on personal, indoor and mobile radio communications. IEEE, 2010.

[10] El-Gohary, N. M., et al. "Utilization of raptor codes for OFDM-system performance enhancing." Wireless Personal Communications 96.4 (2017): 5555-5585.

[11] Koffman and V. Roman, "Broadband wireless access solutions based on OFDM access in IEEE 802.16," in IEEE Communications Magazine, vol. 40, no. 4, pp. 96-103, April 2002, doi: 10.1109/35.995857.

[12] Jankiraman, Mohinder. Space-time codes and MIMO systems. Artech House, 2004.

[13] Delestre, Fabien. Channel Estimation and Performance Analysis of MIMO-OFDM Communications using Space-Time and Space-Frequency Coding Schemes. Diss. 2011.

[14] Ripan Kumar Roy and Tushar Kanti Roy "BER Analysis of MIMO-OFDM System using Alamouti STBC and MRC Diversity Scheme over Rayleigh Multipath Channel".

[15] Sandoval, Francisco, Gwenael Poitau, and François Gagnon. "On optimizing the PAPR of OFDM signals with coding, companding, and MIMO." IEEE Access 7 (2019): 24132-24139.

[16] Neha Therkar and Rohit Rathor "A TECHNICAL REVIEW OF PEAK TO AVERAGE POWER RATIO REDUCTION IN MIMO-OFDM"

[17] Woodard, Jason P., and Lajos Hanzo. "Comparative study of turbo decoding techniques: An overview." IEEE Transactions on vehicular technology 49.6 (2000): 2208-2233.

[18] Bakkas, Brahim, Idriss Chana, and Hussain Ben-Azza. "PAPR reduction in MIMO-OFDM based on polar codes and companding technique." 2019 International Conference on Advanced Communication Technologies and Networking (CommNet). IEEE, 2019.

[19] Chandrasekhar, R., et al. "PAPR reduction using combination of precoding with Mu-Law companding technique for MIMO-OFDM systems." 2015 International Conference on Communications and Signal Processing (ICCSP). IEEE, 2015.

[20] Mohammed, Abdulwahid, et al. "A Novel Companding Technique to Reduce High Peak to Average Power Ratio in OFDM Systems." IEEE Access 9 (2021): 35217-35228.

[21] Zhu, Xiaodong. "A Low-BER Clipping Scheme for PAPR Reduction in STBC MIMO-OFDM Systems." Wireless Personal Communications 65.2 (2012): 335-346.

[22] Singh, Sadhana, and Arvind Kumar. "Performance analysis of adaptive clipping technique for reduction of PAPR in alamouti coded MIMO-OFDM systems." Procedia Computer Science 93 (2016): 609-616.

[23] S. Singh and A. Kumar, "A modified clipping algorithm for reduction of PAPR in OFDM systems," 2015 IEEE International Conference on Computational Intelligence and Computing Research (ICCIC), 2015, pp. 1-4, doi: 10.1109/ICCIC.2015.7435785.

[24] Suzuki, Taku, et al. "Method for generating peak cancellation signals in complexity-reduced PAPR reduction method using null space in MIMO channel for MIMO-OFDM signals." 2019 IEEE VTS Asia Pacific Wireless Communications Symposium (APWCS). IEEE, 2019.

[25] Singh, R. K., and Maniraguha Fidele. "An efficient PAPR reduction scheme for OFDM system using peak windowing and clipping." 2015 Third International Conference on Image Information Processing (ICIIP). IEEE, 2015.

[26] Ni, Chunxing, Yahui Ma, and Tao Jiang. "A novel adaptive tone reservation scheme for PAPR reduction in large-scale multi-user MIMO-OFDM systems." IEEE Wireless Communications Letters 5.5 (2016): 480-483.

[27] Jacklin, Neil, and Zhi Ding. "A linear programming based tone injection algorithm for PAPR reduction of OFDM and linearly precoded systems." IEEE Transactions on Circuits and Systems I: Regular Papers 60.7 (2013): 1937-1945.

[28] Baig, Imran, Varun Jeoti, and Micheal Drieberg. "A ZCMT precoding based STBC MIMO-OFDM system with reduced PAPR." 2011 National Postgraduate Conference. IEEE, 2011.

[29] Pamungkasari, Panca Dewi, et al. "Time domain cyclic selective mapping for PAPR reduction in MIMO-OFDM systems." 2018 IEEE International Conference on Innovative Research and Development (ICIRD). IEEE, 2018.

[30] Jiang, Tao, Chunxing Ni, and Lili Guan. "A novel phase offset SLM scheme for PAPR reduction in Alamouti MIMO-OFDM systems without side information." IEEE signal processing letters 20.4 (2013): 383-386.

[31] Hu, Wei-Wen, et al. "Reduction of papr without side information for sfbc mimo-ofdm systems." IEEE Transactions on Broadcasting 65.2 (2018): 316-325.

[32] Lahcen, Amhaimar, Ahyoud Saida, and Asselman Adel. "Low computational complexity PTS scheme for PAPR reduction of MIMO-OFDM systems." Procedia Engineering 181 (2017): 876-883.

[33] M. Wang, "A Low-Complexity Hybrid Subblock Segmentation PTS Scheme for PAPR Reduction in MIMO-OFDM System," 2020 IEEE 4th Information Technology, Networking, Electronic and Automation Control Conference (ITNEC), 2020, pp. 224-228, doi: 10.1109/ITNEC48623.2020.9085147.

[34] Tsiligkaridis, Theodoros, and Douglas L. Jones. "PAPR reduction performance by active constellation extension for diversity MIMO-OFDM systems." Journal of Electrical and Computer Engineering 2010 (2010).

[35] Ryu, Heung-Gyoon, Sang-Kyun Kim, and Sang-Burm Ryu. "Interleaving method without side information for the PAPR reduction of OFDM system." 2007 International Symposium on Communications and Information Technologies. IEEE, 2007.

[36] Daoud, O., and O. Alani. "PAPR Reduction by Linear Coding Techniques for MIMO-OFDM Systems Performance Improvement: Simulation and Hardware Implementation." European Journal of Scientific Research 36.3 (2009): 376-393.

[37] Mukunthan, P., and P. Dananjayan. "PAPR Reduction based on a Modified PTS with Interleaving and Pulse Shaping method for STBC MIMO-OFDM System." 2012 Third International Conference on Computing, Communication and Networking Technologies (ICCCNT'12). IEEE, 2012.

[38] B. Somasekhar and A. Mallikarjunaprasad, "Modified SLM and PTS approach to reduce PAPR in MIMO OFDM," 2014 International Conference on Electronics, Communication and Computational Engineering (ICECCE), 2014, pp. 245-253, doi: 10.1109/ICECCE.2014.7086621.

[39] Mukunthan, P., and P. Dananjayan. "Modified PTS with FECs for PAPR Reduction in MIMO-OFDM system with different subcarriers." 2011 International Symposium on Humanities, Science and Engineering Research. IEEE, 2011.

[40] Hanzo, Lajos, Tong Hooi Liew, and Bee Leong Yeap. Turbo coding, turbo equalisation and space-time coding. John Wiley and Sons, 2002.

[41] West, Joel. "Commercializing open science: deep space communications as the lead market for Shannon Theory, 1960–73." Journal of Management Studies 45.8 (2008): 1506-1532.

[42] Costello, Daniel J., et al. "Applications of error-control coding." IEEE Transactions on Information Theory 44.6 (1998): 2531-2560.

[43] Roth, Christoph, et al. "Efficient parallel turbo-decoding for high-throughput wireless systems." IEEE Transactions on Circuits and Systems I: Regular Papers 61.6 (2014): 1824-1835.

[44] Boutillon, Emmanuel, Catherine Douillard, and Guido Montorsi. "Iterative decoding of concatenated convolutional codes: Implementation issues." Proceedings of the IEEE 95.6 (2007): 1201-1227.

[45] T. Agrawal, A. Kumar and S. K. Saraswat, "Comparative analysis of convolutional codes based on ML decoding," 2016 2nd International Conference on Communication Control and Intelligent Systems (CCIS), 2016, pp. 41-45, doi: 10.1109/CCIntelS.2016.7878197.

[46] Vaz, Aldrin Claytus, C. Gurudas Nayak, and Dayananda Nayak. "Performance comparison between turbo and polar codes." 2019 3rd International conference on Electronics, Communication and Aerospace Technology (ICECA). IEEE, 2019.

[47] Demjanenko, Victor, Frederic Hirzel, and Juan Torres. "Use of turbo-like codes for QAM modulation using independent I and Q decoding techniques and applications to xDSL systems." U.S. Patent Application No. 09/846,061.

[48] Kim, Youngmin, et al. "A simple soft linear detection for coded multi-input multi-output systems." Wireless Communications and Mobile Computing 13.18 (2013): 1612-1620.

[49] Taskaldiran M., Morling R.C., Kale I. (2009) The Modified Max-Log-MAP Turbo Decoding Algorithm by Extrinsic Information Scaling for Wireless Applications. In: Powell S., Shim J. (eds) Wireless Technology.

Lecture Notes in Electrical Engineering, vol 44. Springer, Boston, MA. https://doi.org/10.1007/978-0-387-71787-6˙13

[50] LaSorte, Nick, W. Justin Barnes, and Hazem H. Refai. "The history of orthogonal frequency division multiplexing." IEEE GLOBECOM 2008-2008 IEEE Global Telecommunications Conference. IEEE, 2008.

[51] Anoh, Kelvin, et al. "A new approach to iterative clipping and filtering PAPR reduction scheme for OFDM systems." IEEE Access 6 (2017): 17533-17544.

[52] Hassan, Emad. Multi-carrier communication systems with examples in MATLAB: A new perspective. CRC Press, 2016.

[53] Sohn and S. C. Kim, "Neural Network Based Simplified Clipping and Filtering Technique for PAPR Reduction of OFDM Signals," in IEEE Communications Letters, vol. 19, no. 8, pp. 1438-1441, Aug. 2015, doi: 10.1109/LCOMM.2015.2441065.

[54] Baltar, Leonardo G., et al. "Computational complexity analysis of advanced physical layers based on multicarrier modulation." 2011 Future Network & Mobile Summit. IEEE, 2011.

[55] Wu, PH-Y. "On the complexity of turbo decoding algorithms." IEEE VTS 53rd Vehicular Technology Conference, Spring 2001. Proceedings (Cat. No. 01CH37202). Vol. 2. IEEE, 2001.

Appendix A

Turbo decoding

The MAP algorithm has been used as a turbo decoder component in order to perform bit-wise soft input soft output estimation. Consider the u_k as the decoded bit at time k and y_k is the received symbol sequence at time k, now reliability measure (LLR) for a single bit at time k under the condition y_k has been received is given by:

$$L\left(u_k\right) = \ln\left(\frac{pr\left(u_k = 1/y_k\right)}{pr\left(u_k = 0/y_k\right)}\right) \tag{A.1}$$

Using Baye's rule of $pr\left(A, B\right) = pr\left(A\right).pr\left(B/A\right)$ the above equation rewritten as:

$$L\left(u_k\right) = \ln\left(\frac{pr\left(u_k = 1, y_k\right)/pr\left(y_k\right)}{pr\left(u_k = 0, y_k\right)/pr\left(y_k\right)}\right) = \ln\left(\frac{pr\left(u_k = 1, y_k\right)}{pr\left(u_k = 0, y_k\right)}\right) \tag{A.2}$$

The probability that u_k becomes 1 or 0 can be expressed in terms of the starting and ending states in the trellis diagram. This depends on the value of the input bit, two-state transitions are available for each of the encoder states. One transition corresponds to the input bit $u_k = 1$ and the other transition corresponds to the input bit $u_k = 0$. Therefore, $pr\left(u_k = 0\right)$ and $pr\left(u_k = 1\right)$ defined by probability for all combinations of starting and ending states that will yield $u_k = 0$ and $u_k = 1$ respectively. Using $pr\left(u_k = 0\right)$ and $pr\left(u_k = 1\right)$ equation (A.2) can rewritten as:

$$L\left(u_k\right) = \ln\left(\frac{\sum_{(s',s)\Rightarrow u_k=1} pr\left(s', s, y_k\right)}{\sum_{(s',s)\Rightarrow u_k=0} pr\left(s', s, y_k\right)}\right) \tag{A.3}$$

The probability to observe a certain pair of states (s', s) depends on the past and the future bits. Therefore, using the received sequence of the past $y_{<k}$, the current y_k, and the future bits $y_{>k}$ and by applying Baye's rule $pr\,(s', s, y_k)$ can express as follows:

$$
\begin{aligned}
pr\,(s', s, y_k) &= pr\,(s', s, y_{<k}, y_k, y_{>k}) \\
&= pr\,(y_{>k}/s', s, y_{<k}, y_k)\,.pr\,(s', s, y_{<k}, y_k) \\
&= pr\,(y_{>k}/s)\,.pr\,(s', s, y_{<k}, y_k) \\
&= pr\,(y_{>k}/s)\,.pr\,(s, y_k/s', y_{<k})\,.pr\,(s', y_{<k}) \\
&= \underbrace{pr\,(y_{>k}/s)}_{\beta_k(s)}\,.\underbrace{pr\,(s, y_k/s')}_{\varphi_k(s',s)}\,.\underbrace{pr\,(s', y_{<k})}_{\alpha_{k-1}(s')}
\end{aligned}
\tag{A.4}
$$

Where $\alpha_{k-1}\,(s')$ is the forward metric, $\varphi_k\,(s', s)$ is transition metric and $\beta_k\,(s)$ is the backward metric. Using these metrics (A.3) express as:

$$
L\,(u_k) = \ln\left(\frac{\sum_{(s',s)\Rightarrow u_k=1} \alpha_{k-1}\,(s')\,.\varphi_k\,(s', s)\,.\beta_k\,(s)}{\sum_{(s',s)\Rightarrow u_k=0} \alpha_{k-1}\,(s')\,.\varphi_k\,(s', s)\,.\beta_k\,(s)}\right)
\tag{A.5}
$$

Transition metric $\varphi_k\,(s', s)$ calculation

$\varphi_k\,(s', s)$ represents the probability that next state is s and the received symbol is y_k given the previous state is s'. $\varphi_k\,(s', s)$ has been calculated using (A.6).

$$
\begin{aligned}
\varphi_k\,(s', s) &= pr\,(y_k, s/s') \\
&= pr\,(y_k/s, s')\,.pr\,(s, s') = pr\,(y_k/x_k)\,pr\,(u_k)
\end{aligned}
\tag{A.6}
$$

Where x_k is the transmitted codeword associated with the state transition from $s_{k-1} = s'$ to $s_k = s$. For the MIMO-OFDM system the transition metric in equation (A.6) already estimated using (4.22).

Forward metric $\alpha_{k-1}\,(s')$ calculation

$\alpha_{k-1}\,(s')$ indicates the joint probability at time $k-1$, the state is s', and the received sequence is $y_{<k}$. $\alpha_{k-1}\,(s')$ calculates using (A.7) in a forward recursion

manner.

$$\alpha_{k-1}\left(s'\right) = pr\left(s', y_{<k}\right)$$
$$\Rightarrow \alpha_k\left(s\right) = pr\left(s, y_{\leq k}\right)$$
$$= pr\left(s, y_k, y_{<k}\right) = \sum_{s'} pr\left(s', s, y_k, y_{<k}\right)$$
$$= \sum_{s'} pr\left(s, y_k/s', y_{<k}\right).pr\left(s', y_{<k}\right) \quad \text{(A.7)}$$
$$= \sum_{s'} \underbrace{pr\left(s, y_k/s'\right)}_{\varphi_k(s',s)} \cdot \underbrace{pr\left(s', y_{<k}\right)}_{\alpha_{k-1}(s')}$$

According to [40] the initial condition for $\alpha_{k-1}\left(s'\right)$ has given by:

$$\alpha_0\left(s\right) = \begin{cases} 1 & for \ \ s = s_0 \\ 0 & for \ s \neq s_0 \end{cases} \quad \text{(A.8)}$$

Where s_0 is the trellis initial state.

Backward metric $\beta_k\left(s\right)$ calculation

$\beta_k\left(s\right)$ represents is the conditional probability that given the current state is s, the future sequence will be $y_{>k}$. This metric has been calculated using backward recursion as follow:

$$\beta_k\left(s\right) = pr\left(y_{>k}/s\right)$$
$$\Rightarrow \beta_{k-1}\left(s'\right) = pr\left(y_{>k-1}/s'\right)$$
$$= \sum_s pr\left(s, y_{>k-1}/s'\right) = \sum_s pr\left(s, y_k, y_{>k}/s'\right) \quad \text{(A.9)}$$
$$= \sum_s pr\left(y_{>k}/s, y_k, s'\right).pr\left(s, y_k/s'\right)$$
$$= \sum_s \underbrace{pr\left(y_{>k}/s\right)}_{\beta_k(s)} \cdot \underbrace{pr\left(s, y_k/s'\right)}_{\varphi_k(s',s)}$$

According to [40] for terminated trellis, the initial condition of $\beta_k\left(s\right)$ has given by:

$$\beta_N\left(s\right) = \begin{cases} 1 & for \ \ s = s_0 \\ 0 & for \ s \neq s_0 \end{cases} \quad \text{(A.10)}$$

Where N is the last stage of the trellis.

The log-MAP algorithm has only slightly more complex than the Max-Log-MAP algorithm, but it gives exactly the same performance as the MAP algorithm [40]. To analyze Log-MAP-based turbo decoding let's define $A_k\left(s\right)$, $B_k\left(s\right)$, and

$\Gamma_k(s',s)$. For rate $\frac{1}{n}$ the branch metric is given by equation (A.11).

$$\Gamma_k(s',s) = \sum_{z=1}^{n} x'_{z,k}.x_{z,k}(s',s) + La_k.u_k(s',s) \tag{A.11}$$

Where $x_{z,k}(s',s)$ and $u_k(s',s)$ denote the zth bit of the codeword and the information bit respectively associated with the state branch (s',s). La_k is the priori value from the component TC decoder and $x'_{z,k}$ is the zth noisy bit-wise soft information for the codeword $x_{z,k}$ which is has been already obtained from the max* operation of (4.21).

$$\begin{aligned} A_k(s) &= \ln(\alpha_k(s)) \\ &= \ln\left(\sum_{s'} \varphi_k(s',s).\alpha_{k-1}(s')\right) \\ &= \ln\left(\sum_{s'} \exp(\Gamma_k(s',s) + A_{k-1}(s'))\right) \\ &= \max_{s'}{}^* (\Gamma_k(s',s) + A_{k-1}(s')) \end{aligned} \tag{A.12}$$

$$\begin{aligned} B_{k-1}(s) &= \ln(\beta_{k-1}(s)) \\ &= \ln\left(\sum_{s} \varphi_k(s',s).\beta_k(s)\right) \\ &= \ln\left(\sum_{s} \exp(\Gamma_k(s',s) + B_k(s))\right) \\ &= \max_{s}{}^* (\Gamma_k(s',s) + B_k(s)) \end{aligned} \tag{A.13}$$

Finally, using $A_k(s)$, $B_{k-1}(s')$, and $\Gamma_k(s',s)$ metrics the Log-MAP of $L(u_k)$ has given by:

$$\begin{aligned} L(u_k) = &\max_{(s',s)\Rightarrow u_k \Rightarrow 1}{}^* (A_{k-1}(s') + \Gamma_k(s',s) + B_k(s)) \\ &- \max_{(s',s)\Rightarrow u_k \Rightarrow 0}{}^* (A_{k-1}(s') + \Gamma_k(s',s) + B_k(s)) \end{aligned} \tag{A.14}$$

Algorithm 1 Log-MAP based STBC detection

$Input: R', H', m, X, \sigma^2$
$Initialization: J = length\left(R'\right), L = zeros\left(m, J\right)$

for $k \leftarrow 1.........J$ **do**
    for $l \leftarrow 1.........m$ **do**
        $S_0 = -\frac{1}{2\sigma^2}\left(\left\|R'\left[k\right] - X_{l\Rightarrow 0}\left[1\right]\right\|^2 + H'\left\|X_{l\Rightarrow 0}\left[1\right]\right\|^2\right)$
        $S_1 = -\frac{1}{2\sigma^2}\left(\left\|R'\left[k\right] - X_{l\Rightarrow 1}\left[1\right]\right\|^2 + H'\left\|X_{l\Rightarrow 1}\left[1\right]\right\|^2\right)$
        for $p \leftarrow 2........2^m$ **do**

$$S_0 \leftarrow \begin{aligned}&\max\left\{S_0, -\frac{1}{2\sigma^2}\left(\left\|R'\left[k\right] - X_{l\Rightarrow 0}\left[p\right]\right\|^2 + H'\left\|X_{l\Rightarrow 0}\left[p\right]\right\|^2\right)\right\} + \\ &\ln\left(1 + \exp\left(-\left|S_0 - \left(-\frac{1}{2\sigma^2}\left(\left\|R'\left[k\right] - X_{l\Rightarrow 0}\left[p\right]\right\|^2 + H'\left\|X_{l\Rightarrow 0}\left[p\right]\right\|^2\right)\right)\right|\right)\right)\end{aligned}$$

$$S_1 \leftarrow \begin{aligned}&\max\left\{S_1, -\frac{1}{2\sigma^2}\left(\left\|R'\left[k\right] - X_{l\Rightarrow 1}\left[p\right]\right\|^2 + H'\left\|X_{l\Rightarrow 1}\left[p\right]\right\|^2\right)\right\} + \\ &\ln\left(1 + \exp\left(-\left|S_1 - \left(-\frac{1}{2\sigma^2}\left(\left\|R'\left[k\right] - X_{l\Rightarrow 1}\left[p\right]\right\|^2 + H'\left\|X_{l\Rightarrow 1}\left[p\right]\right\|^2\right)\right)\right|\right)\right)\end{aligned}$$

        end for
    $Output: L\left(m, k\right) = S_1 - S_0$
    end for
end for